Acta Pharmaceutica Sinica B 2020;10(12):2272–2298

Chinese Pharmaceutical Association
Institute of Materia Medica, Chinese Academy of Medical Sciences

Acta Pharmaceutica Sinica B

www.elsevier.com/locate/apsb
www.sciencedirect.com

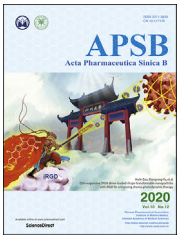

REVIEW

Small molecules targeting the innate immune cGAS–STING–TBK1 signaling pathway

Chunyong Ding[a,b,c], Zilan Song[b,c], Ancheng Shen[b,c], Tingting Chen[b,c], Ao Zhang[a,b,c,*]

[a]*Research Laboratory of Medicinal Chemical Biology & Frontiers on Drug Discovery (RLMCBFDD), School of Pharmacy, Shanghai Jiao Tong University, Shanghai 200240, China*
[b]*CAS Key Laboratory of Receptor Research, Shanghai Institute of Materia Medica (SIMM), Chinese Academy of Sciences, Shanghai 201203, China*
[c]*University of Chinese Academy of Sciences, Beijing 100049, China*

Received 4 December 2019; received in revised form 20 February 2020; accepted 28 February 2020

KEY WORDS

Immunotherapy;
Anti-tumor;

Abstract Multiple cancer immunotherapies including chimeric antigen receptor T cell and immune checkpoint inhibitors (ICIs) have been successfully developed to treat various cancers by motivating the adaptive anti-tumor immunity. Particularly, the checkpoint blockade approach has achieved great

Abbreviations: ABZI, amidobenzimidazole; ACMA, 9-amino-6-chloro-2-methoxyacridine; AMP, adenosine monophosphate; ATP, adenosine triphosphate; BNBC, 6-bromo-*N*-(naphthalen-1-yl)benzo[*d*][1,3]dioxole-5-carboxamide; cAIMP, cyclic adenosine-inosine monophosphate; CBD, cyclic dinucleotide-binding domain; CDA, cyclic diadenosine monophosphate (c-di-AMP); CDG, cyclic diguanosine monophosphate (c-di-GMP); CDN, cyclic dinucleotide; CTLA-4, cytotoxic T lymphocyte associated protein 4; CXCL, chemokine (C-X-C motif) ligand; cGAS, cyclic guanosine monophosphate-adenosine monophosphate synthase; cGAMP, cyclic guanosine monophosphate-adenosine monophosphate; CMA, 10-carboxymethyl-9-acridanone; CTD, C-terminal domain; CTT, C-terminal tail; DC_{50}, concentration for 50% degradation; DCs, dendritic cells; DSDP, dispiro diketopiperzine; dsDNA, double-stranded DNA; DMXAA, 5,6-dimethylxanthenone-4-acetic acid; ENPP1, *ecto*-nucleotide pyrophosphatase/phosphodiesterase; EM, cryo-electron microscopy; ER, endoplasmic reticulum; FAA, flavone-8-acetic acid; FDA, U.S. Food and Drug Administration; FP, fluorescence polarization; GMP, guanosine monophosphate; GTP, guanosine triphosphate; HCQ, hydrochloroquine; HTS, high throughput screening; ICI, immune checkpoint inhibitor; IKK, IκB kinase; IO, immune-oncology; IRF3, interferon regulatory factor 3; i.t., intratumoral; ITC, isothermal titration calorimetry; ISG, interferon stimulated gene; KD, kinase domain; LBD, ligand-binding domain; MDCK, Madin–Darby canine kidney; MG, Mangostin; MI, maximum induction; $MinEC_{5\times}$, minimum effective concentration for inducing 5-fold luciferase activity; MLK, mixed lineage kinase; NF-κB, nuclear factor-κB; Ntase, nucleotidyl transferase; PBMCs, peripheral-blood mononuclear cells; PD-1, programmed death receptor 1; PD-L1, programmed death ligand 1; PDE, phosphodiesterases; PDK1, 3-phosphoinositide-dependent protein kinase 1; PPi, pyrophosphoric acid; PROTACs, proteolysis targeting chimeras; PRRs, pattern recognition receptors; QC, quinacrine; SAR, structure–activity relationship; SDD, scaffold and dimerization domain; STAT, signal transducer and activator of transcription; STING, stimulator of interferon genes; TBK1, TANK-binding kinase 1; THIQCs, tetrahydroisoquinolone acetic acids; TNFRSF, tumor necrosis factor receptor superfamily; ULD, ubiquitin-like domain; VHL, von Hippel–Lindau.

*Corresponding author. Tel./fax: +86 21 50806035.
E-mail address: aozhang@simm.ac.cn (Ao Zhang).

Peer review under responsibility of Institute of Materia Medica, Chinese Academy of Medical Sciences and Chinese Pharmaceutical Association.

https://doi.org/10.1016/j.apsb.2020.03.001

cGAS;
STING;
TBK1;
Small molecule modulators

clinic success as evidenced by several U.S. Food and Drug Administration (FDA)-approved anti-programmed death receptor 1/ligand 1 or anti-cytotoxic T lymphocyte associated protein 4 antibodies. However, the majority of cancers have low clinical response rates to these ICIs due to poor tumor immunogenicity. Indeed, the cyclic guanosine monophosphate-adenosine monophosphate synthase–stimulator of interferon genes–TANK-binding kinase 1 (cGAS–STING–TBK1) axis is now appreciated as the major signaling pathway in innate immune response across different species. Aberrant signaling of this pathway has been closely linked to multiple diseases, including auto-inflammation, virus infection and cancers. In this perspective, we provide an updated review on the latest progress on the development of small molecule modulators targeting the cGAS–STING–TBK1 signaling pathway and their preclinical and clinical use as a new immune stimulatory therapy. Meanwhile, highlights on the clinical candidates, limitations and challenges, as well as future directions in this field are also discussed. Further, small molecule inhibitors targeting this signaling axis and their potential therapeutic use for various indications are discussed as well.

1. Introduction

The human immune system, including adaptive immunity and innate immunity, plays a pivotal role for efficient host defense against foreign genetic invasions. As the first immune barrier, the innate immunity enables the body to fight against pathogen infection through a series of signaling events, including sensing, integration and transmission of non-self or foreign dangerous signals by various pattern recognition receptors (PRRs) in dendritic cells (DCs). As the host cellular proteins, PRRs can recognize pathogen-associated molecular patterns and initiate pro-inflammatory cytokine response and cell-death pathways[1]. The adaptive immunity enables the body possess specific "memory" or long-lasting immune response against the encountered antigens. The innate immune system generally responds quickly to eradicate various foreign dangerous signals, whereas the adaptive immunity is highly dependent on the innate immunity and often requires time to generate a full-blown response.

Immune system has been extensively studied as a critical function during viral invasion and bacterial infection, and its significance in cancer has captured explosive attention in recent years[2]. Tumor can effectively surpass immune response by activating immune homeostasis-associated negative regulatory pathways (checkpoints) to escape deletion. Therefore, immune evasion is a hallmark of cancer, and harnessing the power of the human immune system against cancer has been widely recognized as a tumor-curative approach[2,3]. Indeed, recent years have witnessed multiple cancer immunotherapies successfully developed to treat various cancers, including oncolytic virus, chimeric antigen receptor T cell, bispecific antibodies, and immune checkpoint inhibitors (ICIs), most of which are capable of motivating the adaptive anti-tumor immunity[4,5].

ICIs are designed to target the negative regulatory checkpoint molecules that are expressed in cancer and constrain T cell reactivity or cause exhaustion of the immune system. Therefore, ICIs are expected to restore tumor immuno-surveillance. The approval of the first cytotoxic T lymphocyte associated protein 4 (CTLA-4) inhibitory antibody ipilimumab in 2011[6] and the programmed death receptor 1/ligand 1 (PD-1/PD-L1) antibodies pembrolizumab and nivolumab in 2014[7,8] by the U.S. Food and Drug Administration (FDA) announced the clinical effectiveness of ICIs as a new and revolutionized cancer treatment. Subsequently, enormous efforts have been ignited subsequently for pursuit of more potent and specific next-generation checkpoint inhibitors[9–13], mounting to over ten antibodies receiving regulatory approval worldwide along with over thousands of active clinical trials[14–16]. However, the initial clinical promise of these immune checkpoint blockades is restricted to a small fraction of patients averagely around 20% and to limited tumor types. The majority of patients have minor or no response, and even for the initial responders, a significant number was reported to eventually suffer from relapse due to drug resistance or life-threatening adverse effects, such as cytokine release syndrome and neurotoxicity[17,18]. Therefore, new checkpoint immunotherapies targeting other negative regulators of T cell activation other than PD-1/PD-L1 and CTLA-4 are highly expected, and many of these have already been undergoing clinical trials including those targeting lymphocyte activation gene-3, transmembrane immunoglobulin and mucin domain 3, carcinoembryonic antigen cell adhesion molecule 1, T cell immunoglobulin and ITIM domain, V-domain Ig suppressor of T cell activation, B and T lymphocyte attenuator, and the poliovirus receptor-like receptors CD96 and CD112R[19–21]. Undoubtedly, these approaches will further broaden the horizon of tumor immunotherapy, by not only providing more promising checkpoint inhibitors but also providing a chance to treat a larger number of patients including those untreatable by current therapies.

The checkpoint blockade approach directly targets the adaptive immune system, acting as a controller to release the brakes on anti-tumor T cells[22]. The clinically observed durable anti-tumor effects of the current approved ICIs suggest that these treatable patients have pre-existing T cell-mediated immunity in the tumor (also called "hot" or inflamed tumor), which is deactivated before treatment by checkpoint antibodies. Tumors that are unresponsive to checkpoint inhibitors, especially those immunologically non-inflamed tumors (lack of T cell infiltration, or low or absent of chemokine expression) are "cold" tumors[18,23]. To treat these "cold" tumors and turn them "hot", new immune stimulatory strategies have been developed to activate the innate immune system, thus enhancing tumor immunogenicity[19,24]. In fact, the

majority of cancers in clinic are non-inflamed, and generally have low response rates to current suppressive immunotherapies. Therefore, new type of tumor immunotherapy has been proposed and extensively tested by targeting immune stimulatory molecules, including stimulator of interferon genes (STING), tumor necrosis factor receptor superfamily 4 (TNFSF4, also known as OX40), TNFSF5 (also known as CD40), TNFRSF9, glucocorticoid-induced tumor necrosis factor receptor, and inducible co-stimulator[19,24]. Among these approaches, the recent advance on the development of activators targeting the guanosine monophosphate-adenosine monophosphate synthase–stimulator of interferon genes–TANK-binding kinase 1 (cGAS–STING–TBK1) axis is particularly appealing, and a few candidate compounds have already been undergoing clinical trials[25−28]. Herein, in this perspective, we provide an updated review on the latest progress on the development of small molecule activators targeting the cGAS–STING–TBK1 signaling pathway and their preclinical and clinical trials as a new immune stimulatory therapy. Meanwhile, highlights on the clinical candidates, limitations, challenges, as well as the future directions of this field will be discussed. In addition to activators, inhibitors of this signaling axis and potential therapeutic use for other diseases will also be discussed which will be useful to gain a full interaction landscape of this signaling pathway.

2. The cGAS–STING–TBK1 signaling pathway

STING (also known as TMEM173, MITA, ERIS, and MPYS) is an endoplasmic reticulum (ER) dimeric adaptor protein with 42 kDa 379 amino acids (aa). It contains a transmembrane region (TM1−4, aa 1−154), a cyclic dinucleotide (CDN)-binding domain (CBD, aa 155−341) and a C-terminal tail (CTT, aa 342−379). STING is expressed in various endothelial and epithelial cells, as well as in haematopoietic cells, such as T cells, macrophages and DCs, and acts as a master regulator of type I interferon (IFN) production and the innate immune system[25−28]. In tumor settings, STING is also the major mediator of innate immune sensing of cancerous cells. In normal eukaryotic cells, DNA is strictly packed and separated from cytoplasm to avoid auto-inflammation. However, aberrant localization of DNA in the cytosol occurs due to foreign DNA invasion by either pathogen-derived DNA, self-DNA that leaks from the nucleus of the host cell upon DNA damage, or by DNA infiltration under oxidative mitochondria stress. Presence of these foreign double-stranded DNA (dsDNA) in the cytosol is a dangerous signal to the innate immune system and can be promptly sensed and detected by cyclic guanosine monophosphate (GMP)-adenosine monophosphate (AMP) synthase (cGAS). Subsequent binding of dsDNA with cGAS leads to activation of cGAS and initiates the catalytic synthesis of 2′,3′-cyclic GMP-AMP (cGAMP) from guanosine triphosphate (GTP) and adenosine triphosphate (ATP). As a CDN, 2′,3′-cGAMP contains two distinct phosphodiester linkages, one between 2′-OH of GMP and 5′-phosphate of AMP, and the other between 3′-OH of AMP and 5′-phosphate of GMP. Compared to other endogenous 3′,3′-CDNs from bacteria or virus, the cGAS-synthesized 2′,3′-cGAMP is the endogenous specific ligand that binds and activates STING with high potency. As depicted in Fig. 1, the activated STING is then transported from ER to the Golgi complex, where it recruits the TANK-binding kinase 1 (TBK1) and IκB kinase (IKK), and relocates them to perinuclear regions of the cell. Subsequently, these kinases phosphorylate the transcription factors interferon regulatory factor 3 (IRF3) and nuclear factor-κB (NF-κB) for activation. The incitement of IRF3 and NF-κB triggers the production of type I IFN and many other pro-inflammatory cytokines (Fig. 1)[25−27]. IFNs selectively stimulate cross-presentation of tumor antigens and mobilization of tumor-specific $CD8^+$ T cells, which prime the adaptive immune response against tumors.

The spontaneous sensing and prompt responding toward foreign invading DNA is a fundamental capacity of host defense. However, the underlining intrinsic mechanism remains complex and largely elusive. cGAS, STING and TBK1 are the key effectors involved in host defense, and the cGAS–STING–TBK1 axis is now appreciated as the major signaling pathway in the immune response across different species. Aberrant signaling of this pathway has been closely linked to multiple diseases, and thus it is reasonable to propose that targeting the cGAS–STING–TBK1 pathway would represent a promising immunotherapeutic strategy for treating auto-inflammation, virus infection and cancers[25,26,29−31].

3. Structural determination of the cGAS–STING–TBK1 signaling pathway

3.1. Structural determination and activation mechanism of cGAS

cGAS is the DNA-sensing nucleotidyl transferase (NTase) that can recognize various cytosolic non-self DNA, including various viruses, such as DNA virus and retroviruses, bacterial DNA, and tumor-derived DNA[32]. cGAS consists of an N-terminal tail (aa 1−160) and a NTase domain (aa 161−512). The function of the N-terminal tail is unknown, whereas the NTase domain is crucial for recognition of dsDNA and production of the second messenger 2′,3′-cGAMP[33−35].

The structures of cGAS in complex with dsDNA have been reported from various species. Human and mouse cGAS share 56% identity in amino acid sequences and exhibit similar U-shape structure in the unbound apo state (Fig. 2B)[36]. cGAS can ubiquitously bind with dsDNA from different species through their phosphate backbones, indicating that the binding is non-sequence dependent. Hopfner and co-workers[37] recently found that cGAS preferentially senses longer dsDNA (>20 base pair) with high potency. In the crystal structure of mouse cGAS in complex with a 39 bp dsDNA, two cGAS dimers assemble on two dsDNA in "head-to-head" orientation to form a ladder-like network which has enhanced enzymatic activity (Fig. 2C). They also found that compared to mouse cGAS, human cGAS prefers longer dsDNA due to its two amino acid substitutions in the DNA-binding domain. Therefore, high-order oligomers of cGAS−DNA may exist in mammalian cells or *in vivo*. In addition, the Chen group[34,35] confirmed that cGAS−dsDNA binding is mediated through electrostatic and multiple H-bonds between cGAS's positively charged surface and DNA's sugar-phosphate backbone. Such interactions subsequently induce a significant conformational change of cGAS in the NTase domain, leading to a structural switch of the catalytic pocket to allow binding of ATP and GTP for their cyclization to synthesize 2′,3′-cGAMP. Although

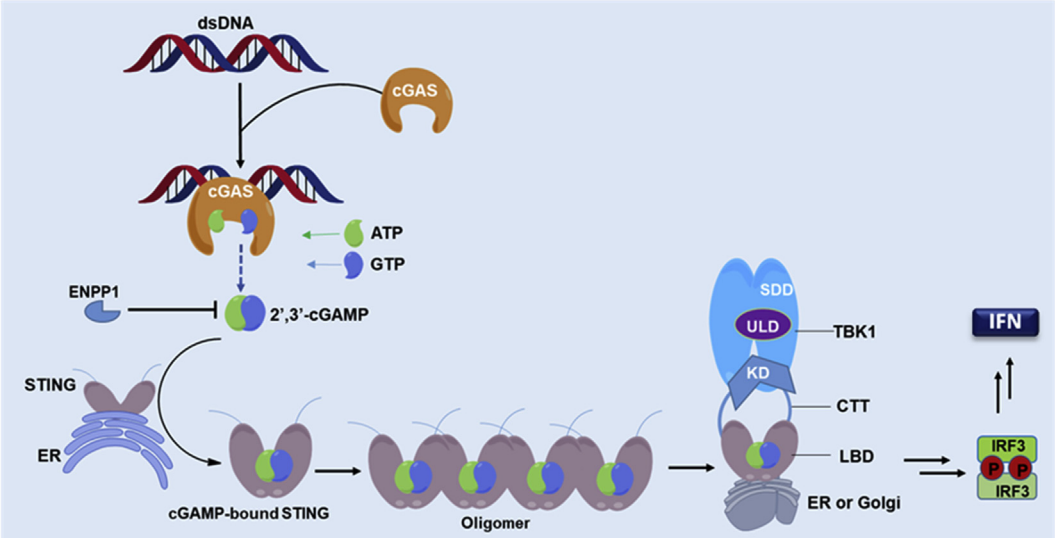

Figure 1 The cGAS–STING–TBK1 signaling pathway. Cytosolic dsDNA is recognized by cGAS, catalyzing the production of cGAMP, which directly binds to the STING dimer on the ER and leads to its activation. The activated STING dimer is then translocated to perinuclear microsome from ER *via* Golgi apparatus, where the C-terminal tail is released leading to STING polymerization. This translocation results in the recruitment and activation of TBK1 by autophosphorylation, which in turn catalyzes the phosphorylation and nuclear translocation of IRF3 to induce transcription of type I IFN genes and other inflammatory genes.

the synthesis of 2′,3′-cGAMP occurs in two steps through a linear dinucleotide intermediate, the exact mechanism for cGAS to preferentially synthesize 2′,3′-cGAMP other than other CDNs (*e.g.*, 2′,2′-cGAMP, 3′,3′-cGAMP and 3′,2′-cGAMP) is still unclear[38,39]. In general, it is proposed that the catalytic activation of cGAS is likely controlled by dsDNA-specific conserved structural switch, which is responsible for the preferred synthesis of 2′,3′-cGAMP to bind with STING[36].

3.2. Structural determination and activation mechanism of STING

STING functions both as an ER adaptor protein sensing cytoplasmic dsDNA and as a direct immunosensor of endogenous CDNs. Human (h) STING and mouse (m) STING share 81% amino acid sequence similarity with 61% identity in the ligand-binding domain (LBD) and exhibit similar structural

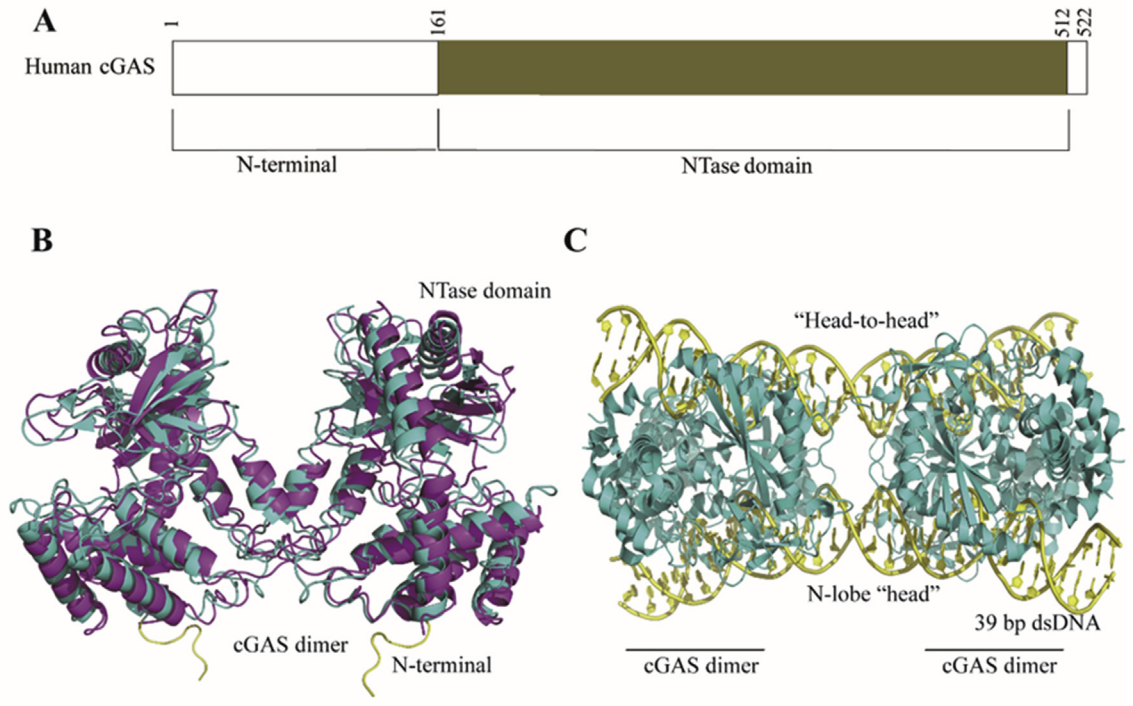

Figure 2 Structural basis of cGAS and its interaction with dsDNA. (A) Human cGAS domain composition. (B) Superimposition of human (colored in cyan, PDB ID: 4LEV) and mouse cGAS (colored in magenta, PDB ID: 4K8V) in apo state. (C) Mouse cGAS in complex with 39 bp dsDNA (PDB ID: 5N6I). cGAS and 39 bp dsDNA are colored in cyan and yellow, respectively.

conformation[26,30–33] (Fig. 3B). hSTING gene is highly heterogeneous and has distinct sequence alleles, including the most common allele R232 with an arginine at amino acid 232, the minor allele H232 with a histidine at amino acid 232, and the second most common human allele HAQ containing triple non-synonymous single nucleotide polymorphisms (R71H-G230A-R293Q). In addition, it was found that ~4% population in Africa are AQ/AQ (R230A-R293Q), which is absent in other ethnic populations. Africans also have the Q293 allele which is likely the founder allele for Africans. Generally, ~30% of East Asians and ~10% of Europeans are HAQ/HAQ, HAQ/H232, or H232/H232. AQ and HAQ might be derived from the founder allele Q293 during the human migration[40].

In view of the central role of STING in the cGAS–STING–TBK1 signaling pathway, the structural study on its apo- and bound-structures would provide fundamental insights in understanding its activation and functioning mechanism[36]. In 2012, the crystal structures of the C-terminal domain (CTD) region of hSTING in its apo (apo-STING^{CTD}) and in complex with cyclic-di-GMP (CDG-bound-STING^{CTD}) were solved by Gu and co-workers[41], respectively, as a similar V-shaped dimer. In the apo-STING^{CTD} structure, two molecules of STING form a V-shaped homodimer with a dimeric interface formed from $\alpha1-\alpha3$ helices and a surface $\alpha2-\alpha3$ loop by van der Waals interaction and multiple H-bonds (Fig. 3B). Similarly, the CDG-bound-STING^{CTD} structure shows a dimeric STING (monomers A and B) in complex with one CDG molecule with 2:1 stoichiometry, and the U-shaped CDG molecule centers in the bottom of the cleft formed by the dimeric STING^{CTD} through multiple H-bonds and stacking interactions (Fig. 3C). Compared to the conformations of the dimeric interface in both structures, there is no significant change in the overall structure of STING^{CTD} upon CDG-binding. However, superposition of both structures indicates a major structural alternation occurring at the $\beta2-\beta3$ loop in the CDG-bound-STING^{CTD} by shifting 1.5–6.3 Å away from the corresponding loop of apo-STING^{CTD}.

Recently, Zhang and co-workers[42] reported the cryo-electron microscopy (EM) structures of full-length STING from human and chicken in the apo state (about 80 kDa in size) and the 2′,3′-cGAMP-bound chicken STING in both the dimeric and tetrameric states. The apo-structures from human and chicken are similar, in which the LBD adopts inactive conformations and the eight transmembrane helices in the STING dimer form a central (TM2 and TM4) and a periphery (TM1 and TM3) layers (Fig. 3D). The cryo-EM structure of 2′,3′-cGAMP-bound chicken STING contains both dimer and higher-order oligomers with a 4:1 ratio. The oligomers predominantly consist of two dimers aggregated in a linear manner through side-by-side packing. The LBD-dimer in full length STING adopts a closed conformation that tightly holds 2′,3′-cGAMP in the ligand-binding pocket (Fig. 3D). Compared to the apo-structure of chicken STING, a 180° rotation is found for the LBD relative to the transmembrane in the cGAMP-bound chicken STING. This rotation is believed to induce a conformational change in a loop on the side of the LBD dimer, leading to tetrameric and higher-ordered oligomeric STING.

Since cGAS-produced 2′,3′-cGAMP and other CDNs, including CDG and cyclic-di-AMP (CDA) from bacteria all activate the STING pathway, Li and coworkers[43] recently conducted an extensive crystal structure study and found that both 2′,3′-cGAMP and CDA, but not CDG, induce the closing of the open apo-STING dimer (Fig. 3E). However, only 2′,3′-cGAMP and CDG directly bind with STING in high potency, whereas the binding affinity of CDA is much weaker (>100 fold less potent than 2′,3′-cGAMP). Further, they confirmed that CDG is able to inhibit cGAMP-induced STING signaling as well. These results indicated that inducing the conformational closing of dimeric hSTING by CDNs is required to achieve higher binding potency, not for STING activation. Meanwhile, the structural study on the hSTING oligomer revealed that binding of cGAMP induces oligomerization of homodimeric STING *via* CTT release, and CTT is requested to protect the polymer interface and prevent auto-activation by facilitating the formation of disulfide-linked polymers *via* Cys 148.

3.3. *Structural determination and activation mechanism of TBK1*

TBK1 is a noncanonical member of IKK family, and plays a key role in the innate immune system. Earlier structural studies suggest that TBK1 exists as a compact dimer containing an N-terminal kinase domain (KD), a ubiquitin-like domain (ULD), and an α-helical scaffold and dimerization domain (SDD, Fig. 4)[44,45]. Upon binding with 2′,3′-cGAMP, STING activates TBK1 and IRF3, leading to the release of type I IFN and many other cytokines[46].

To detect the direct contact of STING with TBK1, Chen and co-workers[47] recently obtained the cryo-EM structure of human TBK1 in complex with cGAMP-bound full-length chicken STING, in which STING was found to form stable oligomers upon 2′,3′-cGAMP binding and release its CTTs. As shown in Fig. 4B and C, the CTTs from the STING oligomers adopt β-strand-like conformations and insert into a groove in the TBK1 dimer formed between the KD of one TBK1 monomer and SDD of another monomer. TBK1 dimer was found to bind STING from the top of cytosolic LBD dimer. However, the transmembrane domain of STING is not involved in the binding interface. Both STING and TBK1 function and signal through phosphorylation, which is induced by 2′,3′-cGAMP-binding, and the binding of STING with TBK1 is enhanced as well by their phosphorylation. In the meantime, Li and co-workers[48] reported a crystal structure of TBK1 bound to human STING, and determined the exact STING residues involved in the binding with TBK1. They found that a highly conserved PLPLRT/SD motif in the C-terminal residues of STING mediates the recruitment of TBK1 by directly binding with the dimeric interface of TBK1. Further analysis of the structure of TBK1 bound to the CTT of STING (STING^{CTT}) revealed that the dimeric TBK1 binds two peptides from STING^{CTT}, and each peptide binds with two TBK1 monomers simultaneously to form a 2:2 complex. It seems that the proximity of TBK1 induced by adjacent STING molecules in the STING oligomers mediates the activation of TBK1. The STING^{CTT} adopts an extended coil structure that binds TBK1 at the PLPLRT/SD motif through hydrophobic interaction and H-bonds (Fig. 4D). All together, these results suggested that 2′,3′-cGAMP-binding initiates activation of STING by formation of stable oligomers, and the PLPLRT/SD motif in the CTT of STING oligomers then binds with the interface of dimeric TBK1 to induce phosphorylation and activation of both STING and TBK1. Further recruitment and

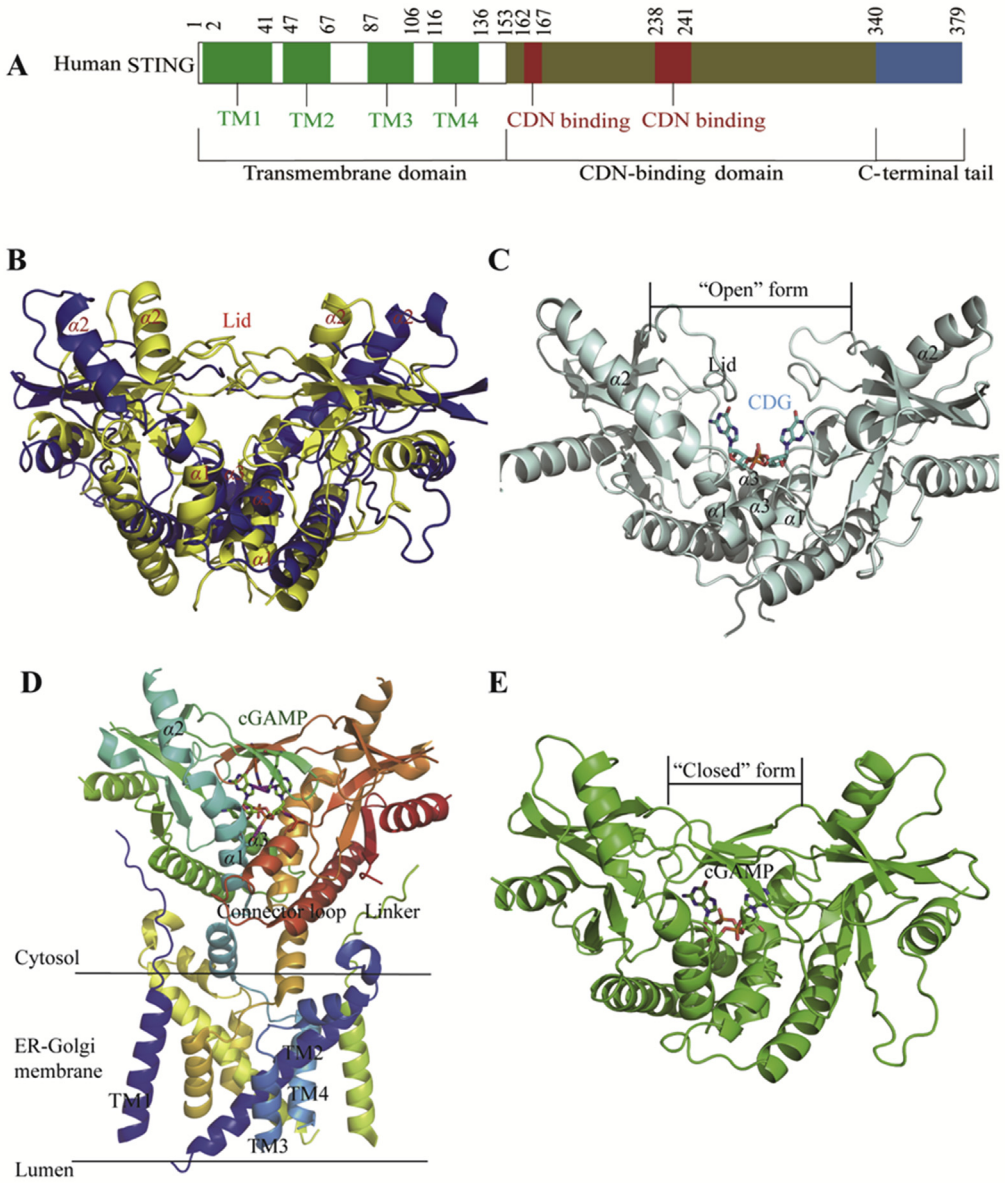

Figure 3 Structural basis of CDN recognition by STING. (A) Human STING domain composition. (B) Superimposition of human (colored in blue, PDB ID: 4EMU) and mouse STING (colored in yellow, PDB ID: 4KCO) in apo state. (C) Human STING (colored in palecyan, PDB ID: 4F5Y) in complex with CDG. (D) Full length chicken STING in 2′,3′-cGAMP-bound state (PDB ID: 6NT7). (E) Human STING in complex with 2′,3′-cGAMP (colored in green, PDB ID: 4LOH).

phosphorylation of IRF3 and TBK1 lead to the engagement of downstream signaling components and regulation of the induction of type I IFN transcription, a hallmark signaling of the cGAS–STING–TBK1 pathway[44–48].

4. Drug development targeting the cGAS–STING–TBK1 signaling pathway

Many types of cancers can induce a spontaneous adaptive T cell response, and foster an immunosuppressive microenvironment favoring its development[49]. Therefore, targeting the cGAS–STING–TBK1 pathway by using agonists to "heat up" tumor microenvironment *via* secretion of IFNs and other cytokines would enhance anti-tumor immune response. Recent years have witnessed the rapid advances in the development of CDN analogues or non-nucleotidyl small molecules as STING agonists to mimetic functions of the endogenous 2′,3′-cGAMP, and many compounds have showed exciting preclinical and clinical benefits[31–35,50–52]. However, agonists targeting cGAS and TBK1 are rare. Meanwhile, inhibitors targeting cGAS–STING–TBK1 have also been developed with potentials for treatment of autoinflammation, virus infection and cancers.

4.1. Development of STING agonists

4.1.1. Natural and synthetic CDNs as direct STING agonists

4.1.1.1. 2′,3′-cGAMP is an endogenous high-affinity STING agonist. The endogenous 2′,3′-cGAMP produced by cGAS in mammalian cells contains two distinct phosphodiester linkages, one between 2′-OH of GMP and 5′-phosphate of AMP, and the other between 3′-OH of AMP and 5′-phosphate of GMP. There are many other similar endogenous CDN analogues with differences

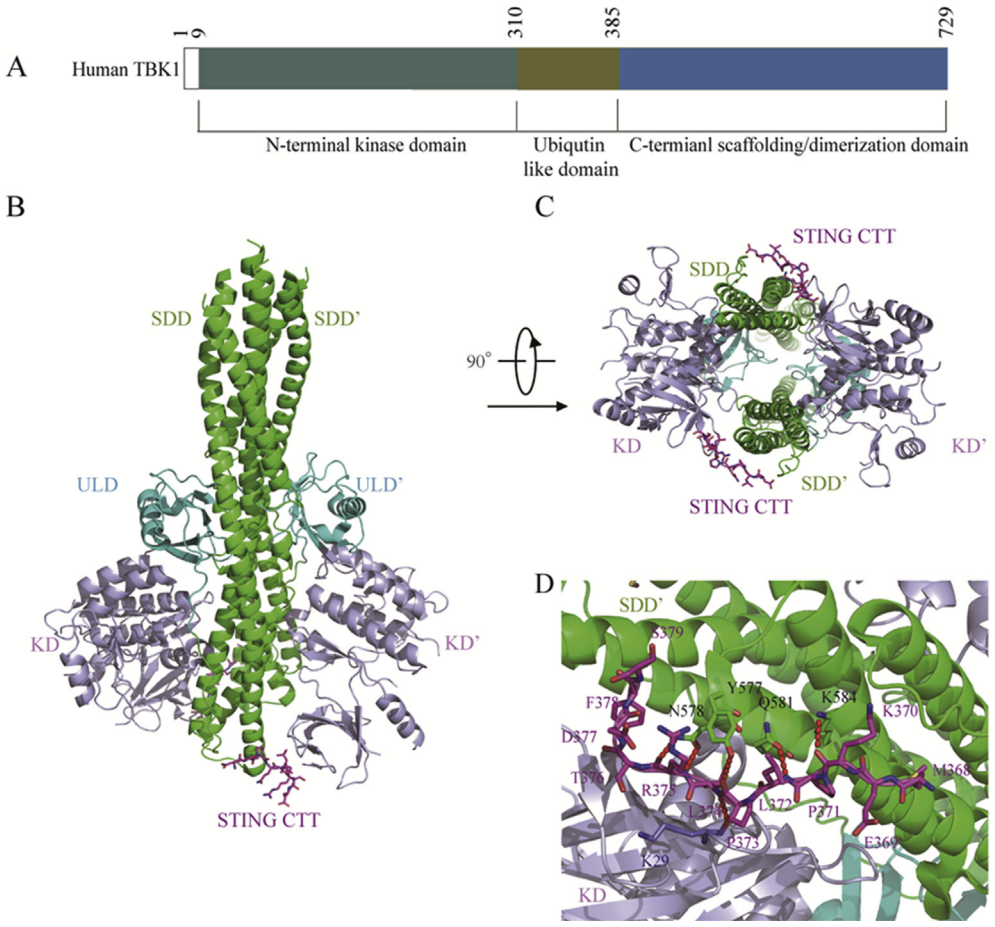

Figure 4 Structural determination of STING/TBK1 complex. (A) Human TBK1 domain composition. (B) and (C) Human TBK1 structure in complex with chicken STING CTT (PDB ID: 6NT9): (B) side view of TBK1, (C) bottom view of TBK1. The conserved motif of STING CTT and the SDD, KD, and ULD of TBK1 are colored in megenta, green, light blue and cyan, respectively. (D) Interaction between the human STING and mouse TBK1 (PDB ID: 6O8C). The conserved motif of STING CTT and the SDD, KD, and ULD of TBK1 are colored in megenta, green, light blue and cyan, respectively. H-bond interactions between STING CTT and TBK1 are depicted as red dashed lines.

only in the phosphodiester linkages. To secure the unique 2′,3′-cGAMP structure preferentially recognized by STING over other cGAMP isomers, Chen et al.[53] chemically synthesized all cGAMPs containing the four possible phosphodiester linkages including 2′,3′-cGAMP, and found that 2′,3′-cGAMP shows distinct difference from other cGAMP isomers in NMR signals of the two anomeric H-1′ (Fig. 5). 2′,3′-cGAMP obtained by chemical total synthesis was confirmed in complete agreement with the one produced by cGAS through stimulation of mouse and human cells with dsDNA in the presence of ATP and GTP substrates by all spectroscopic data. Isothermal titration calorimetry (ITC) experiments showed that the natural agonist 2′,3′-cGAMP binds STING with a K_d value of appropriately 4 nmol/L, which is much lower than other CDN analogues including the other three cGAMP isomers (287 nmol/L to 1.6 μmol/L, Fig. 5) and CDG (1.2 μmol/L). Interestingly, all these cGAMPs induce IFN-β secretion with similar EC_{50} values (16−42 nmol/L), which are much more potent than CDG (>500 nmol/L).

In 2014, Deng et al.[54] reported that treatment with low dosage of 2′,3′-cGAMP (0.5 mg/kg) does not induce appreciable anti-tumor effect, but can enhance anti-tumor immunity induced by radiation. Later, the Tan group[55] conducted a systematic study on both the anti-tumor activity and molecular mechanism of 2′,3′-cGAMP against murine colon 26 adenocarcinoma. They found that the anti-tumor effect of 2′,3′-cGAMP is dose-dependent and an intravenously injected dosage up to 20 mg/kg is able to significantly boost the expression of STING and IRF3, thus producing a tumor inhibition rate up to 60%. Meanwhile, combination of 5-fluorouracil with 2′,3′-cGAMP can potentiate both the anti-tumor effect and the survival rate. Interestingly, 2′,3′-cGAMP still shows modest tumor suppressive activity in *Sting*$^{-/-}$ mice, indicating 2′,3′-cGAMP may stimulate additional pathways other than STING. This result may explain that all the cGAMP isomers in Fig. 5 induce similar levels of IFN-β despite of their distinct binding affinity against STING.

4.1.1.2. ADU-S100 (ML RR-S2 CDA) bearing dithio mixed-linkages. Since the endogenous CDNs including 2′,3′-cGAMP are less active *in vivo* and susceptible to degradation by phosphodiesterases in host cells or in the systemic circulation, Gajewski et al.[56] developed a series of synthetic CDN-derivatives bearing dithio mixed-linkages with both *R*,*R*- and *R*,*S*-dithio diastereomers. The lead molecule **1** (ML RR-S2 CDA, also ADU-S100, Fig. 6) shows improved stability and lipophilicity, and significantly enhances STING signaling by inducing much higher levels of IFN-β than the endogenous 2′,3′-cGAMP and other

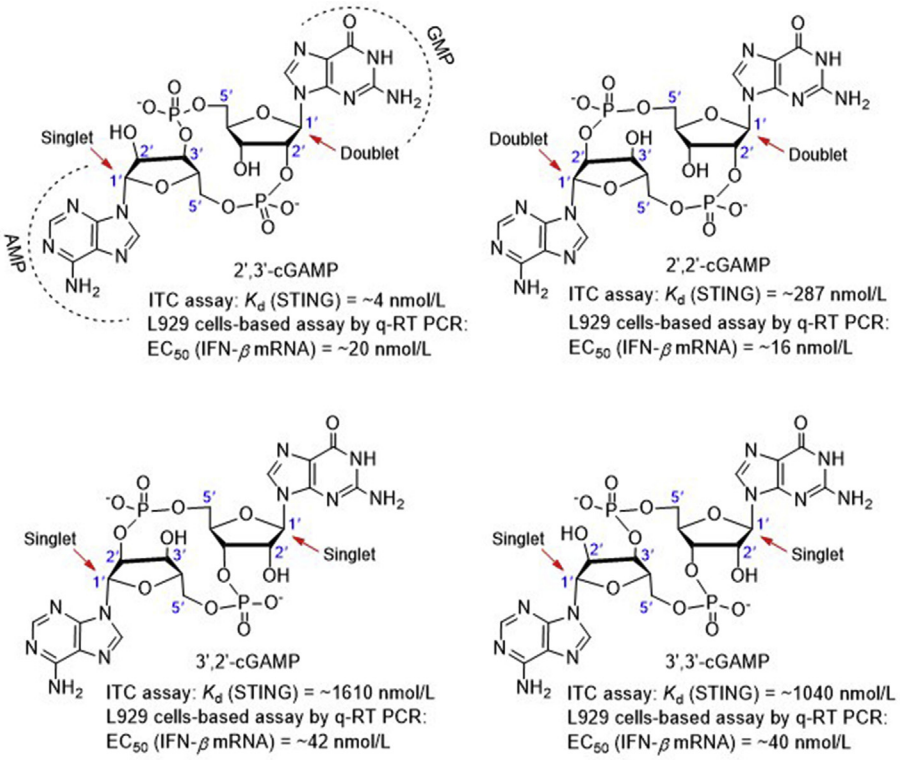

Figure 5 The four natural CDNs (red arrows indicate the H1′ anomeric protons).

pathogen derived CDNs. This synthetic CDN is found to not only activate all known hSTING allelic variants but also show significant tumor growth suppression or regression than the natural STING ligand 2′,3′-cGAMP in several mice models, including BALB/c mice bearing B16 melanoma and BALB/c mice bearing established 4T1 colon or CT26 mammary carcinomas after three 50 μg intratumoral (i.t.) injections. Further, it is found that i.t. injection with ADU-S100 eradicates multiple tumor types and primes an effective systemic $CD8^+$ T cell immune response to suppress the growth of distal untreated tumors. Although the necessity using i.t. injection to achieve maximal therapeutic effect may cause some limitations on the treatment approach, ADU-S100 has been aggressively approached into clinical trials to generate T cell responses against tumor-specific antigens expressed by a patient's individual cancer.

4.1.1.3. Cyclic adenosine-inosine monophosphates (cAIMPs) as potent synthetic CDNs. In 2016, Lioux et al.[57] from InvivoGen reported a series of cAIMP analogues containing one adenosine nucleoside and one inosine nucleoside to replace the two nucleosides (adenosine and guanosine) in the natural CDNs with various sugar moieties (ribose, 2′-deoxyribose, or 2′-fluoro-2′-deoxyribose). These CDNs are also featured by different internucleotide linkage positions (2′,2′; 2′,3′; 3′,3′; or 3′,2′) and phosphate natures (bis-phosphodiester or bis-phosphorothioate, Fig. 6). Many of these cAIMP analogs are found to significantly stimulate the IRF and NF-κB signaling pathways in human and murine immune cell lines. Interestingly, there is no marked difference in the activity between these 3′,3′-cAIMPs and corresponding 2′,3′-isomers. Distinctly different from cAIMPs, natural 2′,3′-cGAMP is much more potent than its 3′,3′-cGAMP isomers to bind STING. In THP1 human monocyte reporter cell (THP1-Dual) lines, the representative cAIMP analogs **2**–**5** induce the greater activation on both IRF production (EC_{50} = 0.3–5.1 μmol/L) and NF-κB signaling (EC_{50} = 1.6–16 μmol/L) than the human 2′,3′-cGAMP (EC_{50} = 7.2 and 39.1 μmol/L, respectively, for IRF and NF-κB). In human blood *ex vivo*, these cAIMPs induce the secretion of IFNs and proinflammatory cytokines with EC_{50} values of 6.4 μmol/L for **2**, 10.6 μmol/L for **3**, 0.7 μmol/L for **4**, and 0.4 μmol/L for **5**, respectively, which are much more potent than 2′,3′-cGAMP (EC_{50} = 19.6 μmol/L). Notably, cAIMPs **4** and **5** containing two 2′-fluoro-2′-deoxyriboses are the most potent in this series in the induction of type I IFNs. Importantly, these cAIMP analogs are more resistant than 2′,3′-cGAMP to the enzymatic cleavage *in vitro*. Particularly, compound **5** shows no degradation even after 2 h incubation with either nuclease P1 or snake venom phosphodiesterase. On the basis of the high *in vitro* potency and stability of these compounds, it would be valuable to test their STING-dependent immunotherapeutic responses *in vivo*.

4.1.1.4. CDN analogue $2'^{AL},3'^{TL}$-cGAMP bearing an uncharged linkage. It is reported that the negatively charged 2′-5′-phosphodiester bond in 2′,3′-cGAMP is the active site for specific degradation by *ecto*-nucleotide pyrophosphatase/phosphodiesterase 1. Carell and co-workers[58] recently designed $2'^{AL},3'^{TL}$-cGAMP (**6**), an analogue of 2′,3′-cGAMP lacking the unique but unstable 2′-5′-phosphodiester linkage. This compound bears a 3′-5′-triazole bond and a 2′-5′-amide bond (Fig. 6), and is obtained by total synthesis in nearly 20 steps with less than 2% overall yield. Unfortunately, this compound is inactive to bind STING.

4.1.2. Non-nucleotidyl small molecule STING agonists

4.1.2.1. mSTING specific small molecule agonists

4.1.2.1.1. 5,6-Dimethylxanthenone-4-acetic acid (DMXAA) and its analogues. The previous clinically failed vascular disrupting agent 5,6-dimethylxanthenone-4-acetic acid **7** (DMXAA, Fig. 7) has been reported as an immune modulator, but the mechanism is

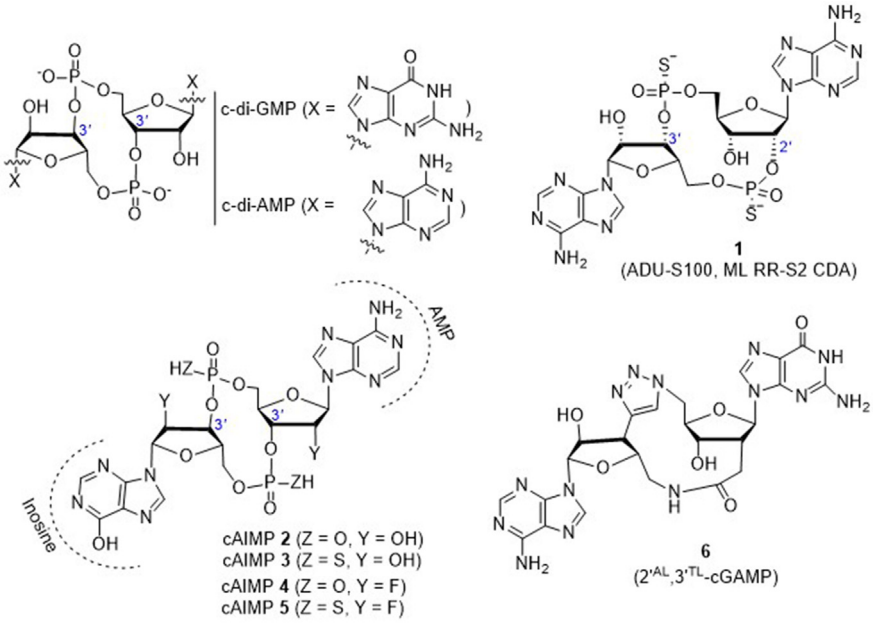

Figure 6 Structures of c-di-GMP, c-di-AMP and the synthetic CDN analogues.

unclear. In 2012, Vogel et al.[59] reported that compound **7** induces the expression of IFN-β in murine macrophages dependent on STING, thus indicating that STING is the target of **7**. Subsequent structure−function studies of mSTING and hSTING revealed that compound **7** is a direct agonist for mSTING, but not hSTING[59,60]. This result at least in part rationalizes the insufficient anti-tumor efficacy observed in the earlier unsuccessful human clinical trials in spite of the high potency in the preclinical mouse study.

To validate the anti-tumor efficacy in mice by directly targeting and activating STING, Gajewski et al.[56] showed that i.t. injection of 500 μg compound **7** effectively primes $CD8^+$ T cell responses and promotes elimination of the established tumors in a STING-dependent fashion. Striking durable disease regression is also observed in multiple mouse tumor models. Based on these proof-of-concept results, compound **7** has been recognized as the prototypic structural model for the development of non-CDN small molecule STING agonists.

In 2014, by combining the structural, biophysical, and cellular assays, Patel and co-workers[61] studied the interaction of compound **7** with mouse and human chimeric proteins of STING. Through point mutations, they identified that compound **7** binds hSTING by forming an inactive "open" conformation, and a single substitution G230I enables the conformation transition to an active "closed" state. The substitution Q266I within the binding pocket that cooperates with G230I together with a point substitution S162A at the binding-pocket was identified as well to render hSTING highly sensitive to compound **7**. On the basis of the complex structure of the engineered hSTING with **7**, especially in view of the large nonpolar hydrophobic pocket formed by Q266, I165, L170 and I235 around the C7 position of compound **7** (Fig. 7), the Han group[62] recently designed a series of C7-substituted analogues with the H-bonding donor or acceptor natures. Compared to compound **7** itself (K_d = 83.4 μmol/L), much weaker binding was observed for all these analogues with the affinity in the order of Br (**8**, K_d = 149 μmol/L) > OH (**9**, K_d = 522 μmol/L) > CH_2OH (**10**) ≫ CH_2CH_2OH (**11**) ∼I (**12**) ∼CHO (**13**) in a thermal shift assay using differential scanning fluorimetry. The highest affinity of 7-bromo analogue **8** is likely due to a strong hydrophobic interaction between the bromine atom and the surrounding I165, I266, L170, and I235 residues. Quite disappointingly, all these analogues fail to show any binding interactions with three tested hSTING variants.

4.1.2.1.2. Other small molecule agonists specifically targeting mSTING. Similar to DMXAA, flavone-8-acetic acid (**14**, FAA), 2,7-bis(2-diethylamino ethoxy)fluoren-9-one (**15**, tilorone), and 10-carboxymethyl-9-acridanone (**16**, CMA) are also the small molecules developed earlier in 1970s as antiviral agents (Fig. 7). Recent studies indicate that these antiviral compounds mediate cell-intrinsic type I IFN responses by activating STING[63]. The more potent compound **16** is confirmed to directly bind STING and trigger a strong antiviral response through the TBK1/IRF3 signaling pathway. However, this extraordinary activity is only observed in mSTING, but not in hSTING-dependent cells. Crystallographic studies showed that two **16** molecules bind to the mouse STING dimer domain in a fashion similar to that of CDG[63].

4.1.2.2. hSTING small molecule agonists

*4.1.2.2.1. Dispiro diketopiperzine **17** (DSDP).* The Chang group[64] recently conducted a high throughput screening (HTS) of 16,000 compounds and identified a dispiro diketopiperzine compound **17** (2,7,2″,2″-dispiro[indene-1″,3″-dione]-tetrahydro dithiazolo[3,2-*a*:3′,2′-*d*]pyrazine-5,10(5a*H*,10a*H*)-dione, Fig. 8) as a cGAS/STING pathway activator. Further study indicated that compound **17** activates a cellular component downstream of cGAS, which is at or upstream of STING. In addition, compound **17** dose-dependently induces the mRNA expression of both type I (IFN-β) and type III (IL-28A and IL-29) IFNs. Interestingly, the induction of cytokine response by compound **17** is dependent on the expression of functional hSTING, but not mSTING.

*4.1.2.2.2. Benzo[b][1,4]thiazine-6-carboxamide **18** (G10) as an indirect STING agonist.* Similarly, through an HTS approach, 4-(2-chloro-6-fluorobenzyl)-*N*-(furan-2-yl methyl)-3-oxo-3,4-dihydro-2*H*-benzo[*b*][1,4]thiazine-6-carboxamide (**18**, Fig. 8)[65] is identified

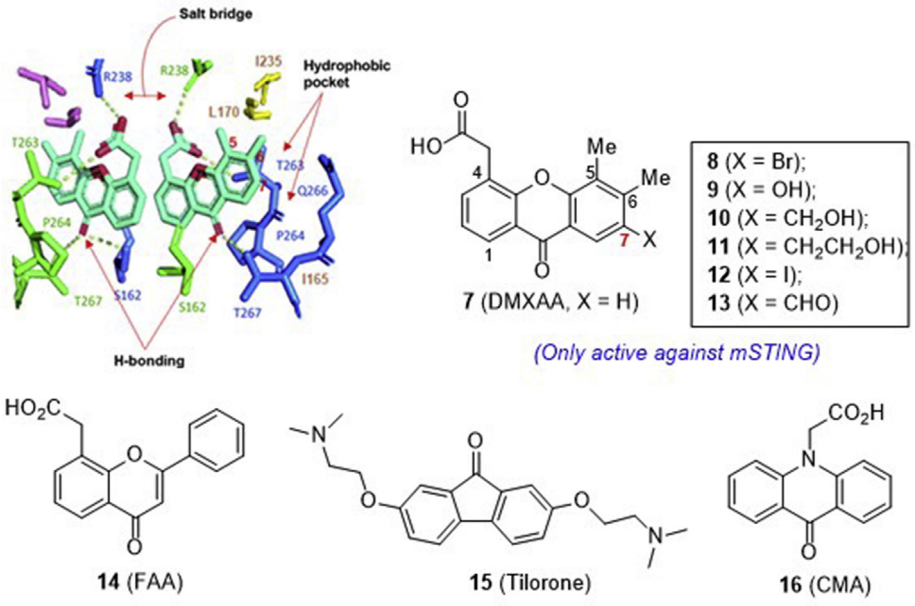

Figure 7 mSTING specific agonists **7**−**16** and co-crystal structure of **7** (DMXAA) bound to murine STING (PDB code 4LOL) with their key intermolecular contacts depicted as green dashed lines.

capable of activating IRF3, but not canonical NF-κB pathways in human fibroblasts. Further examination of the cellular response revealed that compound **18** induces the expressions of multiple IRF3-dependent antiviral effector genes, as well as type I and III IFN subtypes, which promote the cell to prevent the replication of emerging α-virus species. Unfortunately, compound **18** is unable to stimulate the similar activation in murine cells. By employing a reverse genetics approach, IRF3, STING, and the IFN-associated transcription factor STAT1 are found necessary for the observed gene induction and antiviral effects. However, subsequent thermal shift assay indicated that there is no direct binding of compound **18** to STING. Therefore, compound **18** is a synthetic indirect hSTING activator and its potential use needs to be investigated.

*4.1.2.2.3. α-Mangostin (**19**, α-MG) as a hSTING-preferring agonist.* α-Mangostin is a well-known dietary xanthone with moderate anti-tumor and antiviral activities (Fig. 8). Although α-mangostin shares the same xanthone skeleton with DMXAA, Quan and co-workers[66] recently revealed that it is an hSTING agonist with less activity against mSTING. α-Mangostin induces type I IFN production in 293T cells transfected with hSTING plasmids including both $hSTING^{H232}$ and $hSTING^{R232}$ in a dose-dependent manner, and $hSTING^{H232}$ is more sensitive to α-mangostin than $hSTING^{R232}$. The endogenous agonist 2′,3′-cGAMP is found to be a fast-acting STING agonist to induce rapid and robust type I IFN signal that peaks at 2 h, while α-mangostin is a less potent and slow-acting hSTING agonist to induce type I IFN signal peaking at 6 h. Further studies indicated that α-mangostin directly binds and stabilizes $hSTING^{CTD}$, and subsequently enhances the phosphorylation of both TBK1 and IRF3 in a dose- and time-dependent manner, whereas no such effect is observed in *Sting*-knockout THP1 cells[63,66].

*4.1.2.2.4. Benzamide **20** (BNBC) and its analogues **21** and **22**.* 6-Bromo-*N*-(naphthalen-1-yl)benzo[*d*][1,3]dioxole-5-carboxamide (**20**) is a recently identified STING agonist bearing a benzamide framework (Fig. 8)[67]. It induces type I and III IFN dominant cytokine responses in primary human fibroblasts and peripheral-blood mononuclear cells (PBMCs). In addition, compound **20** also induces the cytokine response in PBMC-derived myeloid DCs and promotes their maturation, suggesting that STING agonist treatment can potentially regulate the activation of $CD4^+$ and $CD8^+$ T lymphocytes. Further, compound **20** induces the perinuclear translocation of HepG2 cells expressing hSTING but not those expressing mSTING. A preliminary structure−activity relationship (SAR) study was then conducted, and the minimum effective concentrations to induce 5-fold luciferase activity ($MinEC_{5\times}$) relative to the mock-treated controls and the maximum induction (MI) fold of interferon stimulated gene 54 (ISG54)-promoter activity were tested in HepG2/hSTING cells. It is found that more polar compounds by introduction of an electronegative nitrogen to either the B ring or D ring, or introduction of the water-soluble morpholine to the 2-position of the C ring lead to loss of their activity with $MinEC_{5\times}$ value greater than 200 μmol/L when compared to compound **20** (2.2 μmol/L). In contrast, the A ring opening analogue **21** (57093Z) and D ring opening analogue **22** (57071Z) maintain low $MinEC_{5\times}$ values of 2.5 and 2.6 μmol/L, respectively. Notably, compound **21** has a significantly increased maximum fold of 28.0 to induce ISG54-promoter activity, which is much higher than **20** (20.5-fold) and **22** (17.3-fold) indicating that it might be a more potent STING activator.

4.1.2.2.5. Dimeric amidobenzimidazoles (diABZIs) as a systemic STING agonist. Recently, a HTS program led by Ramanjulu and co-workers[68] at GlaxoSmithKline identified a series of small molecule STING agonists bearing a key amidobenzimidazole (ABZI) component, among which compound **23** shows a moderate inhibitory effect ($IC_{50}^{App} = 14 \pm 2$ μmol/L) against the ^{3}H-cGAMP binding to STING (Fig. 9). The structure of compound **23** in complex with the $STING^{CTD}$ confirms that compound **23** binds in the cGAMP binding pocket with two bound molecules per STING dimer, and each molecule interacts with one STING subunit, spanning the entire side of the pocket without obvious contacts across the dimer interface. Subsequently, they replaced the *N*1-hydroxyphenethyl moiety of the ABZI component with a linker between the two molecules to create a single dimeric ligand diABZI **24**, showing more

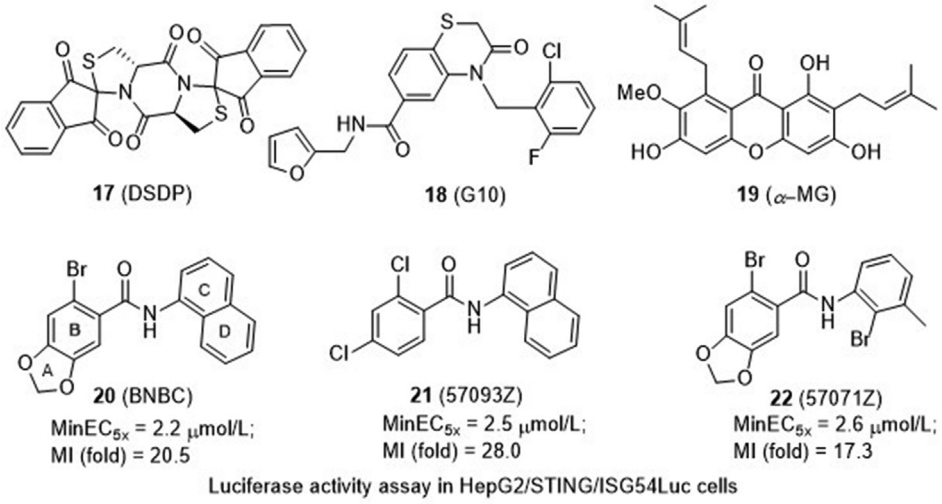

Figure 8 hSTING active small molecule agonists.

than 1000-fold enhanced binding affinity to STING (IC_{50}^{App} = 20 ± 0.8 nmol/L). The complex structure with STING confirms that compound **24** maintains the same protein−ligand contacts as observed with compound **23**, and there is no interaction between the linker and the protein (Fig. 9). Unfortunately, compound **24** induces a moderate secretion of IFN-β (EC_{50}^{app} = 3.1 ± 0.6 μmol/L), thus encouraging a further structural optimization to improve cell membrane permeability. Finally, diABZI **25** is identified retaining high binding affinity with improved potency in primary cells and functional activity across different human haplotypes and mouse STING. In human PBMCs, compound **25** induces the dose-dependent activation of STING and the secretion of IFN-β with an EC_{50}^{app} value of 130 nmol/L. It exhibits optimal systemic exposure with a half-life time of 1.4 h and satisfactory plasma concentrations. Intermittent dosing of **25** at 1.5 mg/kg intravenously in subcutaneous CT-26 tumors results in the significant tumor growth inhibition as measured by tumor volume AUC analysis ($P < 0.001$), and significantly improves survival ($P < 0.001$) with 8 out of 10 mice remaining tumor free at the end of the study (Day 43). Interestingly, unlike cGAMP and DMXAA, these diABZIs efficiently activate STING function while maintaining an open STING confirmation. Based on these studies, diABZI **25** represents the first intravenously efficacious non-CDN STING agonist with systemic anti-tumor activity, and is warranted for further preclinical or clinical study.

In addition to the patent from GlaxoSmithKline, recently scientists from the HITGEN[69] at China also disclosed a series of diABZIs either by replacing the benzoimidazole component in diABZI **25** with an imidazopyrimidine motif or replacing the solvent−interaction alkoxy groups with other groups (Fig. 9). The representative compounds **26**−**28** show low micromolar binding affinity to STING (K_d = 1−3 μmol/L) and high potency (EC_{50} = 8.6−330 nmol/L) in the induction of chemokine (C-X-C motif) ligand-10 (CXCL-10) in PBMC cells. Particularly, intermittent injection of compound **26** either intratumorally or intraperitoneally shows significant tumor growth inhibition or regression in BALB/c mice bearing established CT26 mammary carcinomas.

4.1.2.2.6. Bicyclic benzamides. Recently, Curade Pharm[70−72] at India disclosed three patents claiming three series of bicyclic benzamides as potent STING agonists (Fig. 10). Representative compounds of the first series include 3-oxo-3,4-dihydro-2*H*-benzo[*b*][1,4]thiazine-6-carboxamide (**29**), 2-oxo-2,3-dihydro-1*H*-pyrido[2,3-*b*][1,4]thiazine-7-carboxamide (**30**), and 2-oxo-1,2,3,4-tetrahydroquinoline-7-carboxamide (**31**)[70]. All these compounds have micromolar range of activity in the HEK293T-hSTING luciferase assay, and potently induce the secretion of IFN-α/β, IL-6, CXCL-10, and TNF-α in human PBMC cells. In the BALB/c mice bearing R232 hSTING-expressed CT26 tumor, i.t. injections of all the three compounds at 200 μg dosage thrice a week induce significant tumor growth suppression. Compounds **29** and **30** are more potent than **31**, suggesting a contribution of the ring heteroatoms N or S. 2-Oxo-1,2,3,4-tetrahydroquinazoline-7-carboxamides **32**−**34** represent the second series of compounds and also show significant activation effects on STING[71]. I.t. injections of these three compounds at 200 μg dosage thrice a week introduce significant tumor growth inhibition. Especially, compound **34** nearly completely suppresses the tumor growth. Compounds **35**−**37** represent the third series of compounds bearing a 2-oxoindoline-6-carboxamide skeleton, and show similar potency in hSTING activation assays[72]. Similarly, these compounds induce significant tumor growth suppression in BALB/c mice bearing established CT26 tumor.

4.1.2.2.7. Benzothiophene derivatives. Merck Sharp & Dohme Corp.[73] recently claimed a series of multi-substituted benzothiophenes **38** (Fig. 11) as STING agonists. The 4-oxobutanoic acid side chain is important for the activity, and subtle alternations on the phenyl cause significant difference in potency. It is found that the conformation of the cyclopropane moiety within the side change is also important, and the *cis*-isomer **39** is less potent than *trans*-isomer **40** with EC_{50} values of 114 and 703 nmol/L, respectively, in the STING-binding assay. Interestingly, despite the moderate binding affinity (mostly in micromolar range), compounds **41**−**43** show significant functional activity with percent activation (% effect) several folds higher than 2′,3′-cGAMP in IFN-β secretion of THP1 cells. Although the *in vivo* anti-tumor efficacy is not disclosed in this patent, recently two additional patents from Merck[74] further claimed that these benzothiphene compounds have significant STING-dependent anti-tumor activity in advanced MC38 mouse syngeneic tumor model with i.t. intermittent injection, and clinical study in the treatment

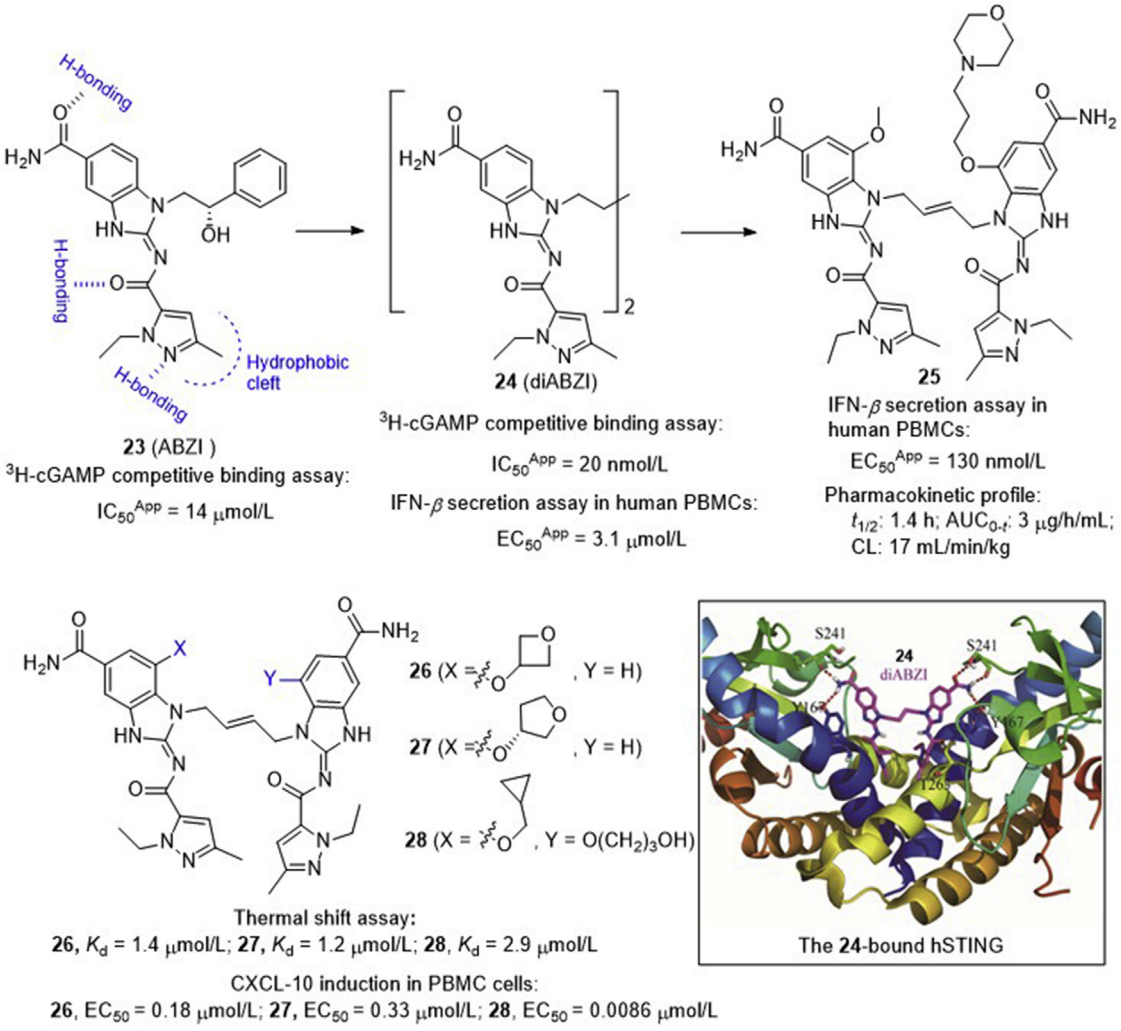

Figure 9 Development of diABZIs as potent systemic STING agonists and co-crystal structure of diABZI **24** bound to human STING (PDB ID: 6DXL). Red dashed lines depict the key H-bond interactions of diABZI **24** with human STING.

of patients with advanced/metastatic solid tumors or lymphomas had been proposed either alone or in combination with anti-PD-1 antibodies[75].

4.2. *Development of STING inhibitors*

4.2.1. *Tetrahydroisoquinolone acetic acids (THIQCs)*

Since earlier structural analysis of 2′,3′-cGAMP in complex with $STING^{CTD}$ indicated that the binding of the agonist induces the apo state STING to transition from an "open" conformation to a "closed" conformation[41]. Therefore, stabilization of the "open" conformation would lead to inactivation of STING, whereas stabilization of the "closed" conformation might lead to activation of the protein. Based on the large binding pocket of STING, Siu and co-workers[76] recently established a robust platform to identify STING inhibitors, and 1-oxo-1,2,3,4-tetrahydroisoquinolin-4-yl carboxylic acid (**44**, Fig. 12A) was initially obtained as a low activity hit with an IC_{50} value of 7300 nmol/L in the HAQ STING-cGAMP displacement assay. The easy one-pot synthesis of this compound led to subsequent generation of diverse derivatives, providing compound **45** as a high potent STING inhibitor with an IC_{50} value of 84 nmol/L. To improve the poor pharmacokinetic properties of **45** (calculated $pK_a = 4.3$; oral bioavailability, $F = 5\%$; permeability, MDCK $P_{app} = 9 \times 10^{-6}$ cm/s), extension of the carboxylic acid to the homologated acid provides THIQC **46** that has slightly higher potency ($IC_{50} = 68$ nmol/L) and much improved oral bioavailability of 60% with high intrinsic clearance. Co-crystal structure of **46** bound to STING protein confirms that this compound binds in a 2:1 ratio to the STING homodimer in the "open" inactive conformation (Fig. 12B). Since stabilizing the "open" conformation is proposed to prevent all STING signaling, THP1 cells were then incubated with **45** and **46**, respectively, with or without cGAMP stimulation, and no significant stimulation of IFN-β production ($EC_{50} \geq 30$ μmol/L) were observed. Intriguingly, functional study indicated that the inhibition of the cGAMP-induced IFN-β production by either compounds **45** ($IC_{50} = 11.5$ μmol/L) or **46** ($IC_{50} = 11.0$ μmol/L) is unexpectedly modest, which is over 100-fold less potent compared to their binding affinity.

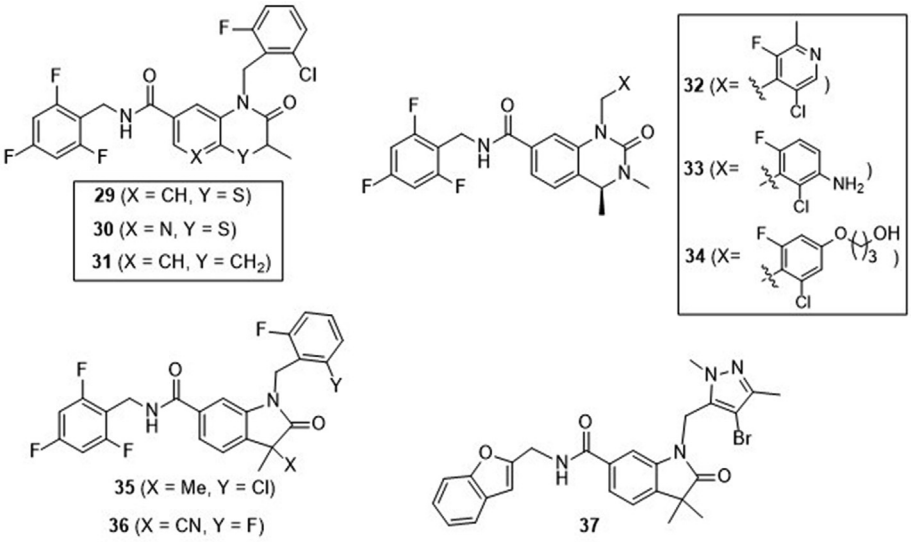

Figure 10 Bicyclic benzamides from patents of Curade Pharm.

4.2.2. Small molecule covalent inhibitors

Recently, Ablasser and co-workers[77] from IFM Therapeutics performed a cell-based chemical screening and identified a series of compounds as covalent inhibitors of STING (Fig. 13). First, two nitrofuran derivatives **47** and **48** were found to strongly reduce STING-mediated IFN-β reporter activity. Their high selectivity is confirmed by broad reduction of 498 (99.6%) of the 500 most-upregulated genes induced by a STING agonist. Mechanism study suggested that these compounds covalently target the predicted transmembrane Cys 91 thereby blocking the activation-induced palmitoylation of STING. The species-specific study suggested that the two compounds directly target mSTING but not hSTING. Further SAR study indicated that the nitrofuran moiety and the central amido NH are critical for the inhibitory activity and the *N*-methyl analogue **49** is inactive. Meanwhile, two additional compounds **50** and **51** were identified to efficiently inhibit both hSTING and mSTING through the same mechanism of action. Meanwhile, a new urido compound **52** was also found as a potent hSTING inhibitor, which is depended on Cys91 as well. Notably, pretreatment with **52** markedly reduces systemic cytokine responses in the sting agonist-treated mice. Trex-1 is the most abundant 3′,5′-exonuclease in mammalian cells that digests cytosolic DNA. Mutation or deletion of *TREX* gene in humans can cause several autoimmune diseases. Compound **52** exhibits marked efficacy in *Trex1*$^{-/-}$ mice expressing a bioluminescent IFN-β reporter. Therefore, this compound is a highly potent and selective small molecule antagonist of STING that has noteworthy inhibitory activity both *in vitro* and *in vivo*.

4.2.3. Natural cyclopeptide Astin C and its analogue

Wang and co-workers[78] recently isolated a series of natural chlorinated cyclopentapeptides from roots and rhizomes of the traditional Chinese medicinal plant *Aster tataricus*. Compositae-type cyclopeptides consist of one proteinogenic amino acid (L-Ser) and four nonproteinogenic amino acids, such as L-β-Phe, L-Abu, L-*allo*-Thr, and chlorinated L-Pro derivatives. Among them, the cyclopeptide Astin C (**53**, Fig. 13) bearing a unique 3,4-dichloropyrrolidine-2-carboxylic acid moiety exhibits potent

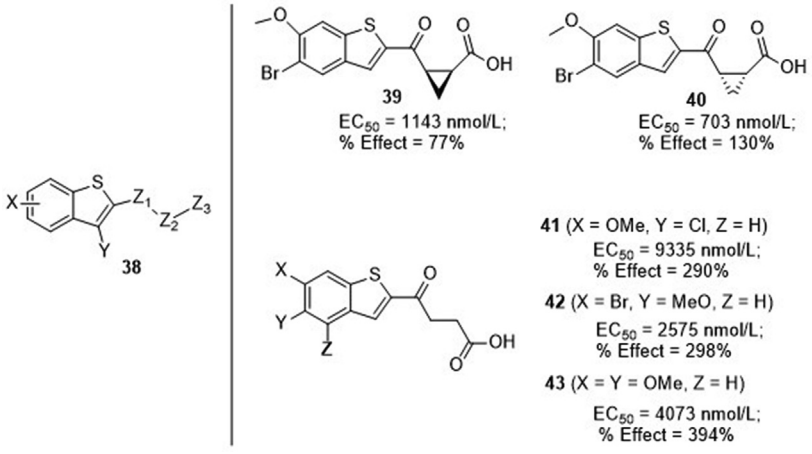

Figure 11 Benzothiophene derivatives from patents of Merck. EC_{50} values were obtained from ^{3}H-cGAMP filtration binding assay, and % effect values represent the ability to induce IFN-β secretion in THP-1 cells relative to 2′,3′-cGAMP at 30 μmol/L.

and specific activity in blocking STING-dependent signaling with IC_{50} values of 3.42 ± 0.13 and 10.83 ± 1.88 μmol/L, respectively, for m- and h-STING fibroblasts, whereas the analogue **54** without the 3,4-dichloropyrrolidine component is inactive. Compound **53** binds $STING^{CTD}$-H232 with a K_d value of 2.37 ± 0.38 μmol/L, roughly equivalent to that of the endogenous CDNs (K_d for CDG, 2.77 ± 0.54 μmol/L; K_d for 2′,3′-cGAMP, 2.18 ± 0.32 μmol/L). Further mutagenesis analysis revealed that compound **53** specifically targets STING and competes with CDNs for binding the C-terminal activation pocket of STING. To facilitate *in vivo* study, compound **53** complexed with hydroxypropyl β-cyclodextrin was prepared to improve the water solubility and this complex was delivered into mice *via* tail vein injection once every 2 days. Administration of the complex consistently and strongly inhibited the mRNA expression of IFN-β, CXL10, ISG15, ISG56, and TNF-α, and alleviated the auto-inflammatory symptoms in *Trex1*$^{-/-}$ bone marrow-derived macrophages and STING-mediated disease animal model[78].

4.3. Development of cGAS inhibitors

As the cytosolic DNA sensor, cGAS is a critical alarming molecule to detect invading dangerous pathogens. However, persistent activation of cGAS can cause autoimmune diseases, such as Aicardi-Goutieres syndrome and lupus. Therefore, manipulating cGAS may pave a new avenue for treatment of acute or chronic inflammatory diseases through modulation of the cGAS−STING pathway. Although activation of cGAS can produce significant signaling amplification, development of cGAS agonists proves to be challenging. Alternatively, several research groups have reported the progress on the development of cGAS inhibitors, which may be useful as potential treatment of autoimmune disease[25,34,35].

4.3.1. cGAS indirect inhibitors

4.3.1.1. DNA intercalators as indirect cGAS inhibitors. In 2016, Hammond and coworkers[79] reported their development of an RNA-based fluorescent biosensor, which allowed for high throughput screening of cGAS inhibitors by quantifying the levels of cellular 2′,3′-cGAMP produced by cGAS. From their compound library, they found that anti-malarial drug quinacrine hydrochloride (**55**) and fluorescent probe ethidium bromide (**56**, Fig. 14), both previously used as DNA intercalators, show full inhibition of cGAS activity at 100 μmol/L, and RNA polymerase inhibitor actinomycin D (**57**) shows partial inhibition. Therefore, nucleic acid intercalators are a class of cGAS inhibitors, which likely act indirectly by intercalating and shifting DNA helix conformation and interfering DNA−cGAS binding.

4.3.1.2. Repurposing antimalarial drugs as indirect GAS inhibitors. By *in silico* prediction based on a mouse cGAS-DNA co-crystal structure, Elkon and co-workers[80] identified a series of antimalarial drugs bearing aminoacridine or aminoquinolone scaffold as new cGAS inhibitors (Fig. 15). Among these, quinacrine (QC, **58**), 9-amino-6-chloro-2-methoxyacridine (ACMA, **59**) and hydrochloroquine (HCQ, **60**) are found to be the most potent with IC_{50} values of 13−354 μmol/L for inhibiting the synthesis of 2′,3′-cGAMP to prevent IFN-β production in THP1 cells. Subsequent studies confirmed that these compounds dose-dependently disrupt the DNA−cGAS complex, likely by inserting into the DNA's minor groove of the DNA−cGAS interface, to indirectly impair DNA-stimulated cGAS activity. Further, several *N*-alkylated analogues were prepared, and the resulting 3-amino acridines **61**−**63** (Fig. 15) show compatible activity, but compound **63** has the optimal aqueous solubility and cell penetration with less cytotoxicity[81]. Therefore, compound **63** was further tested in the *Trex1*$^{-/-}$ mice developing a severe type I IFN-dependent inflammatory myocarditis. Since these drugs have

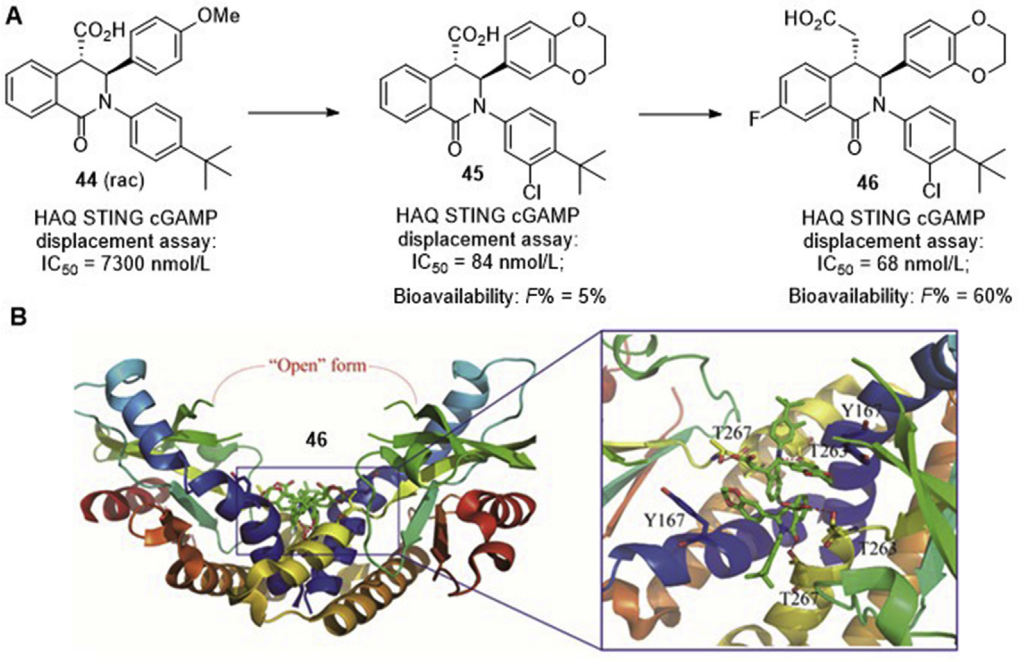

Figure 12 (A) hSTING inhibitors **44**−**46** bearing 1-oxo-tetrahydroisoquinolin-4-yl carboxylic acid fragment; (B) co-crystal structure of human STING in complex with compound **46** (PDB ID: 6MEX), and red dashed lines depict their key interactions.

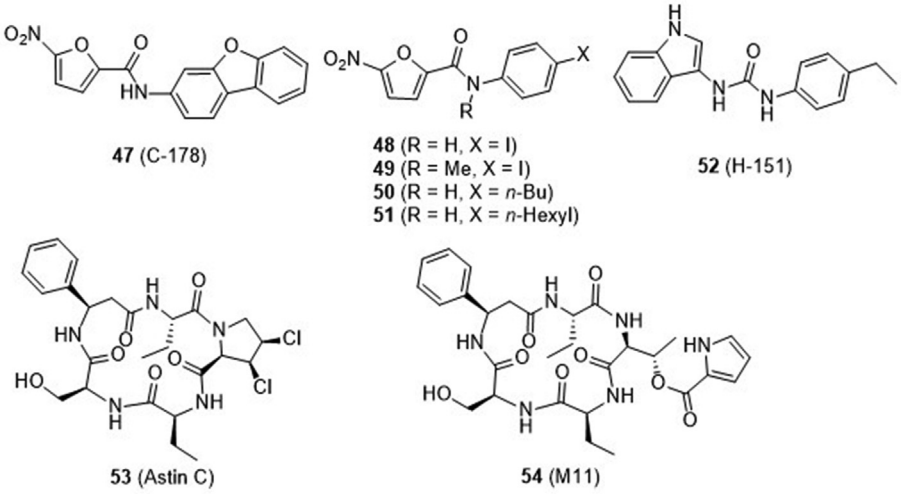

Figure 13 Covalent inhibitors **47**−**52** and natural macrocyclic peptides **53** and **54**.

already been clinically prescribed, further modification focusing on improving cGAS activity would lead to potent druggable cGAS inhibitors.

4.3.1.3. DNA mimic compound suramin as an indirect cGAS inhibitor. Through HPLC-based medium throughput screening of 268 compounds library, Sintim and co-workers[82] identified the river blindness and African sleeping sickness drug suramin (**64**) as an inhibitor of cGAS (Fig. 15). It dose-dependently inhibits the synthesis of 2′,3′-cGAMP and downregulates the production of IFN-β in THP1 cells. It is found that suramin does not directly bind DNA, but likely disrupt the dsDNA-cGAS binding through acting as a DNA displacement without cGAS activation function.

4.3.2. cGAS direct inhibitors

4.3.2.1. Mouse- and/or human-specific direct inhibitor of cGAS. Using a mass-spectrum based HTS assay, Ascano et al.[83] screened a library of over 1000 compounds for their inhibitory effects on mouse cGAS (m-cGAS) to inhibit the production of 2′,3′-cGAMP, leading to four compounds **65**−**68** showing IC_{50} values of 110−1890 nmol/L (Fig. 16). The co-crystal structure of the representative compound **65** (RU365, IC_{50} = 1.89 μmol/L) in complex with dsDNA and cGAS was obtained. Structural analysis and subsequent point mutations showed that this compound adopts an active conformation in the DNA-induced "open pocket", similar to that of 2′,3′-cGAMP with cGAS. The benzimidazole ring and portion of the pyrazole ring in compound **65** partially stack with Arg 364 and Tyr 421, forming the key intermolecular interactions. Further structural modification led to the dichloro compound **66** (RU521) showing much improved activity (IC_{50} = 0.11 μmol/L) against cGAS catalytic activity. The crystal structure shows that the two chloro moieties in compound **66** insert deeper in the catalytic pocket of cGAS that increases the stacking surface of the compound with Arg 364 and Tyr 421 (Fig. 17A). Kinetic analysis showed that compound **66** occupies the catalytic site of cGAS, thus blocking its binding with ATP and GTP, the two substrates for synthesis of 2′,3′-cGAMP. In the murine RAW macrophage cells, treatment with compound **66** reduces cGAS-dependent IFN induction with an IC_{50} value of 0.7 μmol/L. Unfortunately, despite the high biochemical and cellular activity together with high cGAS selectivity, compound **66** is only active against m-cGAS (IC_{50} = 0.11 μmol/L), but not against human cGAS (h-cGAS, IC_{50} = 2.94 μmol/L). Since m- and h-cGAS share 60% amino acid identity, an alternative method for characterization of h-cGAS inhibitors is needed.

To obtain direct h-cGAS inhibitors, Tuschi et al.[84] recently established a fast and more costive screening strategy of h-cGAS specific inhibitors. Using this method, they successfully identified two hit compounds **69** (J001) and **72** (G001) showing IC_{50} values of 1−2 μmol/L against h-cGAS, but these two hits are 2- to 4-fold less potent than m-cGAS (Fig. 16). Subsequently, they conducted a medicinal chemistry optimization campaign to boost h-cGAS activity and selectivity based on both hit compounds. Optimization of hit **69** leads to the identification of **70** as the most potent m- and h-cGAS inhibitors with IC_{50} values of 100 and 60 nmol/L, respectively. However, the cellular potency is much lower in both cGAS mRNA-expressing human monocytic THP1 (IC_{50} = 2.63 μmol/L) and mouse macrophage RAW 264.7 (IC_{50} = 3.58 μmol/L) cells. Compound **71** lacking the nitro moiety is much less potent than **70**, indicating the nitro group is essential for cGAS activity. Considering that nitroarenes generally have carcinogenic and genotoxic liability, further modification of this series was terminated. Structural optimization of the pyridoindole tricyclic chemotype **72** led to a number of compounds with different selectivity for either m- or h-cGAS (Fig. 16). It is found that the *ortho*-dichloro substitution pattern on the indole phenyl ring prefers to recognize h-cGAS, and the representative compounds **73**−**75** show high biochemical potency against h-cGAS with IC_{50} values of 28.0, 14.0 and 10.0 nmol/L, respectively. An additional substituent on the indole phenyl has a minor effect on h-cGAS, but can alter the h-/m-cGAS selectivity. 3-Amino-pyrid-6-yl substituted compound **75** (G150) is the most potent and selective h-cGAS inhibitor but is inactive against m-cGAS (IC_{50} > 25 μmol/L). The crystal structure of compound **75** in complex with apo h-cGAS catalytic domain (h-$cGAS^{CD}$, K427E/K428E) indicates that this compound partially occupies the binding pockets of ATP and GTP, and forms several key interacts between $cGAS^{CD}$ and the dichloroindole, 2-aminopyridine, and the hydroxyacetamide components (Fig. 17B). In the THP1 cells, the highly potent h-cGAS specific inhibitors **73**−**75** show

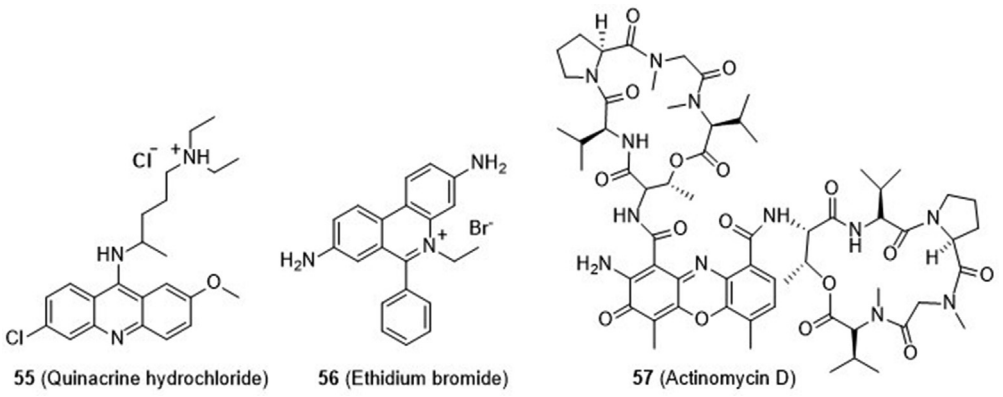

Figure 14 Nucleic acid intercalators **56** and **57** as indirect cGAS inhibitors.

dose-dependent inhibitory effects against the expression of *IFNB1* mRNA with IC_{50} values of 2.95, 1.70 and 1.96 μmol/L, respectively. In spite of the lower cellular potency, the high biochemical activity together with the high cGAS dependency and h-cGAS selectivity make these compounds valuable for further studies.

4.3.2.2. cGAS direct inhibitor PF-06928215. Through fragment-based ^{1}H-NMR screening, scientists at Pfizer[85] identified a hit compound tetrazolo[1,5-*a*]pyrimidin-7-ol (**76**) showing cGAS binding affinity of 171 μmol/L (K_d) in the surface plasmon resonance (SPR) assay and functional inhibition of 78 μmol/L (IC_{50}) in the fluorescence polarization (FP)-based assay (Fig. 18). The crystal structure of this compound in complex with cGAS shows that it occupies a binding site similar to that of the adenine base in either ATP or 2′,3′-cGAMP. Compound **76** is instable to readily undergo ring-opening, and then isomerize to **77**. A scaffold-hopping approach was then conducted leading to a series of 7-hydroxy-5-phenylpyrazolo[1,5-*a*]pyrimidine-3-carboxamides **78**–**80** with improved stability. The *N*-methyl amide **78** retains modest binding affinity again cGAS (K_d = 78 μmol/L), but the affinities of analogues **79** and **80** are significantly improved with K_d values of 2.7 and 0.2 μmol/L, respectively. Both compounds show good functional activity with IC_{50} values of 17.5 and 4.9 μmol/L, respectively. Intriguingly, despite the high biochemical and functional potency, the most potent compound **80** (PF-06928215) fails to show detectable activity in cellular cGAS assay measuring dsDNA-induced IFN-β expression, and the underlying reason is unclear.

4.3.2.3. Pyrazolopyrimidinones as cGAS inhibitors. Aduro Biotech[86] recently disclosed a large series of pyrazolopyrimidinones as cGAS inhibitors (Fig. 19). Among these, compounds **81**–**83** are the representative compounds in each subseries, showing IC_{50} values less than 20 μmol/L in the

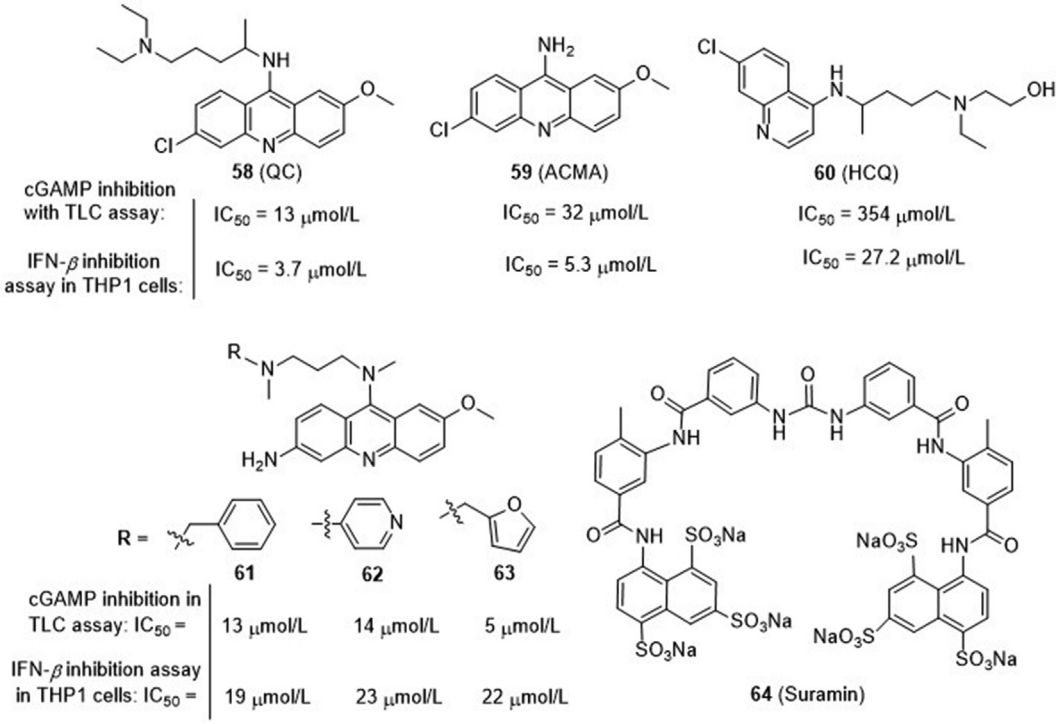

Figure 15 Repurposing antimalarial and antivirus drugs as indirect cGAS inhibitors.

suppression of cGAMP production. More specifically, compound **82** containing 4-methoxybenzo[*d*]oxazol-2-yl as the *C*6-substituent in the pyrazolopyrimidinone core displays appreciable inhibitory effect on the secretion of cytokines CCL5 and CCL2 in cGAS-dependent THP1 cells with IC_{50} values of 1.25 and 6.93 μmol/L, respectively. However, the underlying mechanism for inhibition of cGAS activity is not mentioned.

4.4. *Development of TBK1 inhibitors*

Since aberrant regulation of TBK1 has been reported to be implicated in the induction of antiviral innate immune response and tumor migration/progression, TBK1 has been proposed as a drug target for drug development against multiple diseases related to the cGAS–STING–TBK1 pathway[44–46]. On one hand, virus invading is an important activation pathway of TBK1, which might be useful for host to boost its immune system against virus. On the other hand, over-activation of TBK1 may cause the progression of many diseases, including autoimmune, cancer and obesity. Therefore, inhibitors of TBK1 would provide a potential treatment of these diseases. Since it is challenging to develop direct activators of a kinase such as TBK1, numerous efforts have been devoted to the screening and characterization of TBK1 inhibitors[44–46,87].

2,4-Diaminopyrimidine **84** (BX795, Fig. 20) is the earliest TBK1 inhibitor reported in 2009 with an IC_{50} value of 6.0 nmol/L[88]. This compound is originally developed as a modest potent inhibitor of 3-phosphoinositide-dependent protein kinase 1 (PDK1, IC_{50} = 111 nmol/L), but also shows high potency against a number of other kinases including IKKε, Aurora B, MLK1−3 (mixed lineage kinase 1−3), and MARK1−4 (AMP-activated protein kinase 1−4) with IC_{50} values of 5−100 nmol/L. The multi-kinase profile of compound **84** is likely ascribed to its 2,4-aminopyrimidine core that forms key interactions in the hinge binding region of many APT-competitive kinases through H-bondings with the pyrimidine *N*1 and the 2-amino substituents. Compounds **85** (MRT67307)[89] and **86** (CYT387)[90] are among the earlier selective TBK1 inhibitors. Compound **85** is derived from **84** with improved selectivity for TBK1 (IC_{50} = 19 nmol/L) and IKKε (IC_{50} = 160 nmol/L) over other kinases, whereas compound **86** is repurposed from momelotinib, a clinically prescribed JAK1/2 inhibitor for treatment of myelofibrosis. Since all of these earlier TBK1 inhibitors bear a central aminopyrimidine framework, subsequently many research groups both from academia and industry spent tremendous efforts to generate more potent and selective analogues. The work published before 2014 has been highlighted by Cho and co-workers[87]. Notably, aminopyrimidines **87**−**90** represent the highly potent TBK1 inhibitors with IC_{50} values less than 2 nmol/L. Compounds **87** and **88** developed by Domainex[91] are over 200-fold more potent for TBK1 than IKKβ, JNK-1 and JNK-3, and are able to inhibit the secretion of a number of pro-inflammatory cytokines in inflammatory disease mouse model. Similarly, compounds **89** and **90** developed by the Scripps Research Institute[92] are TBK1 specific inhibitors (IC_{50} < 1 nmol/L), showing distinct suppression of tumor cell proliferation and tumor development in the xenograft and allograft mice (100 mg/kg, daily i.p.).

To identify new potent and selective TBK1 inhibitors to probe the function of TBK1-involving signaling pathway, Rauh and co-

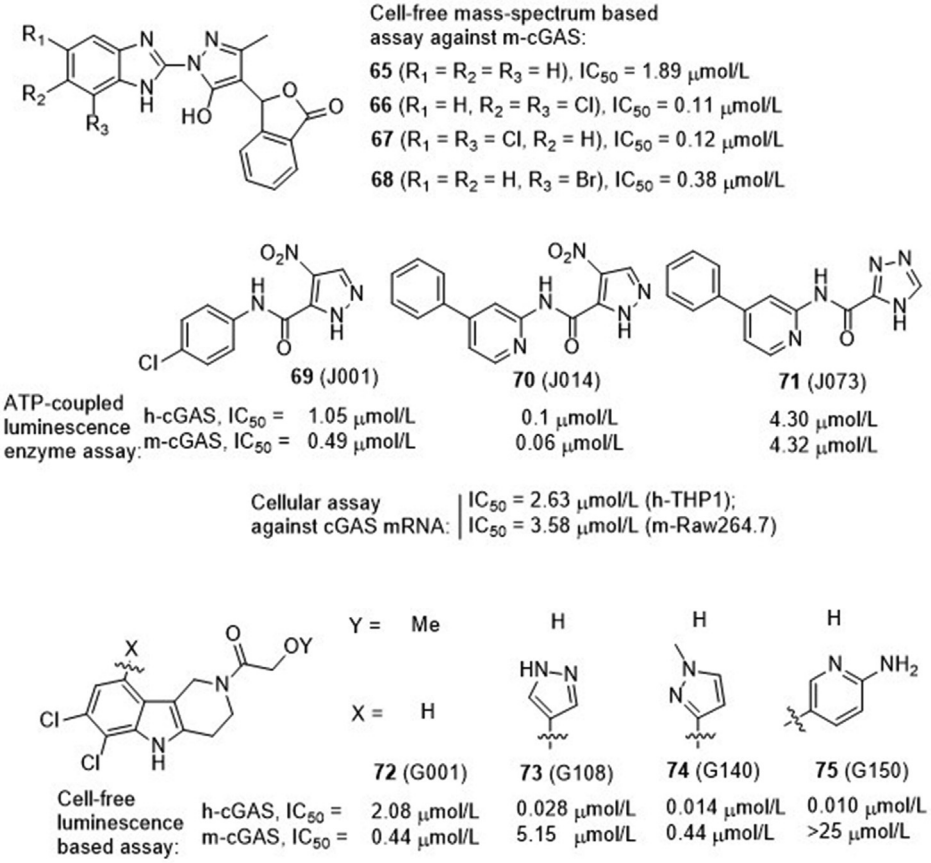

Figure 16 cGAS direct inhibitors **65**−**75**.

workers[93] conducted an activity-based assay of a large compound library from GSK, ROCHE as well as their own in-house collection. This approach led to identification of many clinically used kinases inhibitors showing high potency against TBK1, including K252a (IC_{50} < 1 nmol/L), dovitinib (IC_{50} = 60 nmol/L), oxindole **91** (IC_{50} = 3 nmol/L) as well as many other aminopyrimidines (Fig. 21). Since these compounds can form similar H-bonding network as compound **84** in the kinase hinge binding region, it is not surprising that they generally act as multi-target inhibitors including TBK1. Subsequently, they focused on the Aurora kinase inhibitor tozasertib that shows moderate potency for TBK1 (IC_{50} = 6.22 μmol/L) and established a traceable SAR, leading to identification of the more potent TBK1 inhibitors **92**–**94** (Fig. 21). Interestingly, the most potent compound **92** with an IC_{50} value of 60 nmol/L, nearly 100-fold more potent than the prototypic compound tozasertib, fails to show effect on the IFN production in RAW macrophages, whereas significant suppressive effects are observed in the cases of the less potent compounds **93** (IC_{50} = 340 nmol/L) and **94** (IC_{50} = 840 nmol/L).

Amlexanox (**95**, Fig. 22), an FDA-approved drug for asthma and aphthous ulcer, is recently found showing modest activity against TBK1 with an IC_{50} value of 0.8 μmol/L. Since chronic low-grade inflammatory is a hallmark of obesity and type 2 diabetes, this drug is further tested in clinic and shows positive response to a subset of obesity and diabetic patients. Encouraged by this result, Tesmer and co-workers[94] resolved the crystal structure of amlexanox in complex with TBK1 showing the hinge region binding of the aminopyridine fragment in the kinase catalytic domain (Fig. 23). Subsequently, a series of analogues were synthesized focusing on the replacement of the *C*3-carboxylic moiety. Elimination of the acid moiety or its conversion to amides leads to the reduced potency, whereas the bioisosteric tetrazole **96** shows increased potency with an IC_{50} value of 400 nmol/L. Unfortunately, this compound has lower aqueous solubility than amlexanox, and fails to significantly increase both pTBK1 response and gene expression of IL-6. Recently, Showalter and co-workers[95] reported a large series of analogues by replacement of the *C*7-isopropyl of amlexanox, among which a few compounds have compatible or slightly improved potency against TBK1. The representative compounds **97** and **98** are further tested in 3T3-L1 adipocytes, and both of them significantly enhance the phosphorylation of TBK1 and IL-6 secretion.

Bergamini and co-workers[96] from the GlaxoSmithKline recently reported a highly selective TBK1 inhibitor GSK8612 (**99**, Fig. 22), which also bears a central aminopyrimidine chemotype. It shows a high binding affinity of 10 nmol/L (K_d), and no off-targets are identified within 10-fold affinity range. In addition to its high aqueous solubility and cellular permeability, this compound inhibits IRF3 phosphorylation in Ramos cells, and

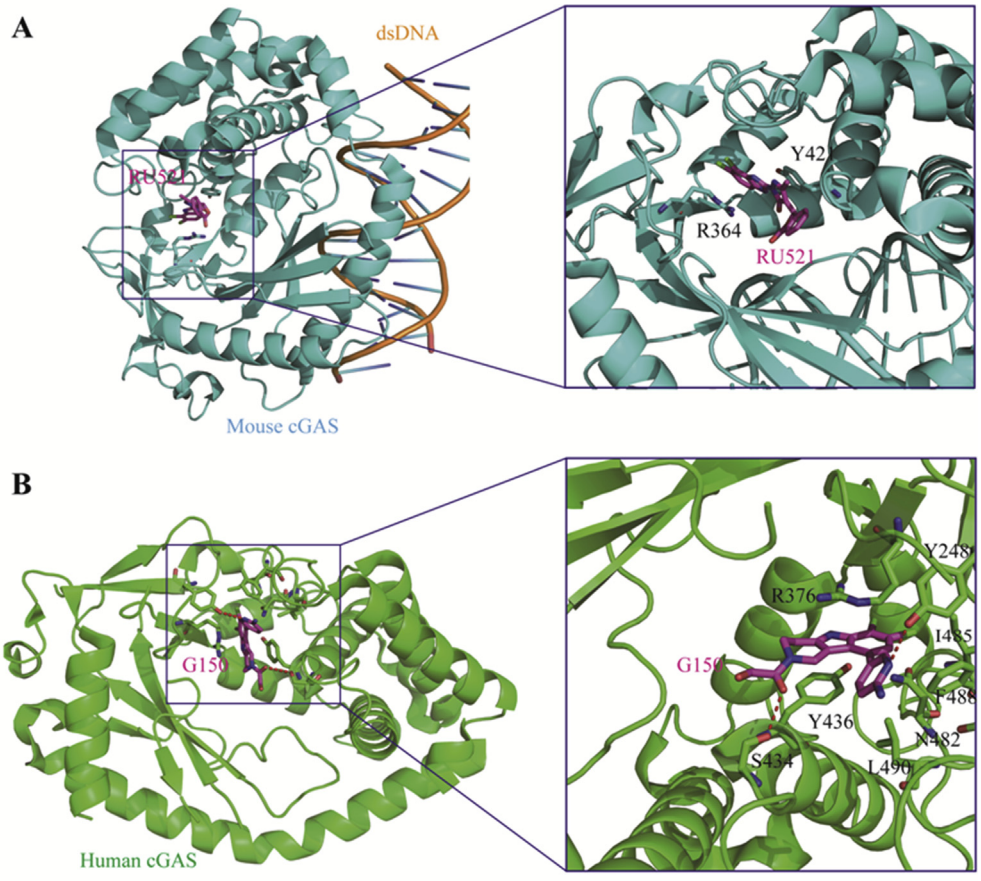

Figure 17 (A) Co-crystal structure of m-cGAS in complex with **66** (RU521, PDB ID: 5XZG). The m-cGAS and **66** are colored in cyan and magenta, respectively. (B) Co-crystal structure of h-cGAS catalytic domain in complex with **75** (G150, PDB ID: 6MJW). The human cGAS and **75** were depicted in green and magenta, and H-bonds are depicted as red dashed lines.

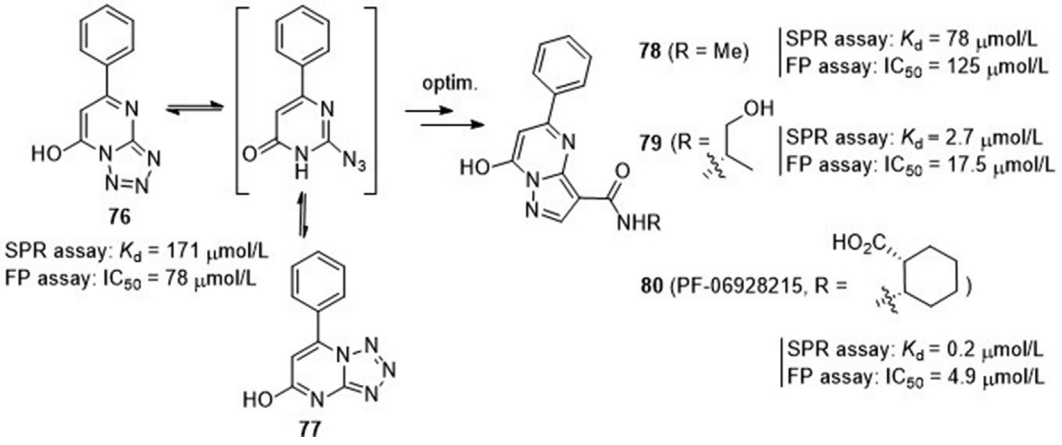

Figure 18 Discovery of cGAS direct inhibitor PF-06928215.

suppresses the secretion of IFN-β in THP1 cells stimulated with 2′,3′-cGAMP or ds-DNA-containing virus.

Recently, Crews and co-workers[97] developed a series of proteolysis targeting chimeras (PROTACs) as TBK1 degraders (Fig. 24). The TBK1 inhibitor 2,4-diaminopyrimidine **100** with a binding K_d value of 1.3 nmol/L and the von Hippel−Lindau (VHL) E3 ubiquitin ligase binder hydroxyproline **101** with an IC_{50} value of 800 nmol/L were selected as the model to be connected through a flexible oxygen-containing linker. It is found that a linker with greater than 12-atom is essential for achieving over 90% degradation. The representative compound **102** bearing a 15-atom linker retains potent TBK1 binding affinity with a K_d value of 4.6 nmol/L and degradation with a DC_{50} (concentration for 50% degradation) value of 12 nmol/L. Further modification of the pyrimidine *C*5-bromo of the TBK1 binder led to compound **103** with both stronger binding potency (K_d = 4 nmol/L) and degradation activity (DC_{50} = 3 nmol/L) toward TBK1. However, optimization of the *t*-butyl moiety of the VHL ligand portion did not provide better compounds with sufficient degradation of TBK1. The potential of the PROTACs is further confirmed in several cancer cell lines harboring wild-type or mutant K-RAS and PROTAC **102** shows complete degradation of TBK1 in both cell types without significant difference.

4.5. Development of ecto-nucleotide pyrophosphatase/phosphodiesterase 1 (ENPP1) inhibitors

ENPP1 is a type II transmembrane glycoprotein, which hydrolyzes extracellular ATP to AMP and pyrophosphoric acid (PPi). The produced AMP is then metabolized by the *ecto*-5′-nucleotidase CD73 to the immuno-suppressive adenosine, whereas the diphosphate PPi is an inhibitor of bone mineralization. Inactivating mutations and overexpression of ENPP1 have been reported in various diseases including cancer[98,99]. However, the role of this enzyme in the dsDNA/cGAS/STING innate immune pathway is not clear. To this end, Mitchison and co-workers[99] conducted a systemic study through activity-guided fractionation to identify the key hydrolase for specific degradation of 2′,3′-cGAMP, which may be used as an alternative potential drug target to modulate the cGAS–STING–TBK1 pathway. First, they ruled out the 11 classes of phosphodiesterases (PDE1−11) that are known as hydrolytic enzymes for the cleavage of 3′−5′-phosphodiester bond in cAMP and cGMP, as well as PDE12 that is the only known PDE for hydrolysis of 2′−5′-phosphodiester bond. Subsequently, ENPP1 was identified as the dominant and direct 2′,3′-cGAMP hydrolase in cells, tissue extracts, and blood. This enzyme has similar hydrolysis

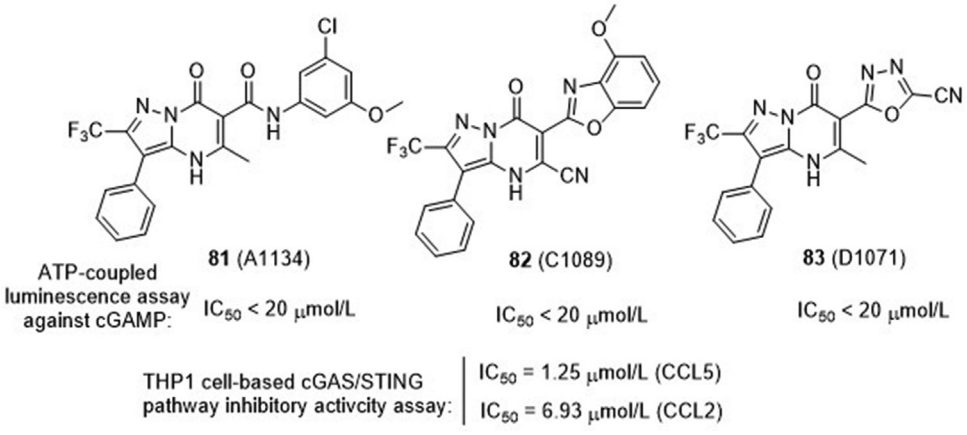

Figure 19 Pyrazolopyrimidinones from ADURO Biotech.

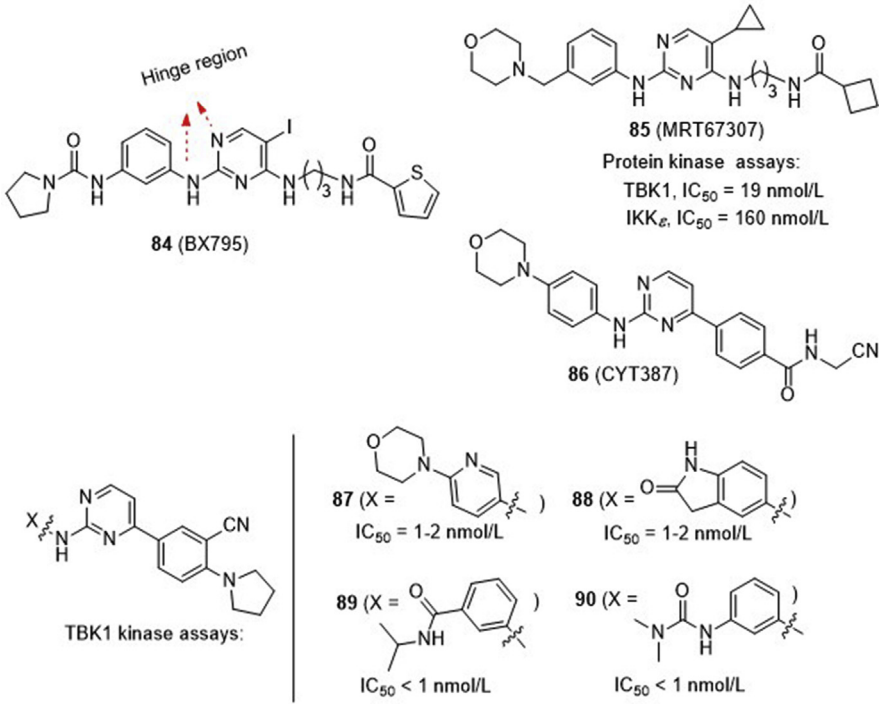

Figure 20 Earlier developed TBK1 inhibitors (before 2014).

potency for 2′,3′-cGAMP (K_m = 15 μmol/L, K_{cat} = 4 s^{-1}), compared to the substrate ATP (K_m = 20 μmol/L, K_{cat} = 124 s^{-1}). Since the phosphodiester 2′,3′-cGAMP is instable and the corresponding phosphothioate diester congeners are generally believed to be more stable and resistant to the hydrolysis by PDEs and nucleases. Therefore, a few phosphothioate analogues of 2′,3′-cGAMP were enzymatically synthesized by either replacing the 3′-5′-phosphodiester bond (**104**, 2′,3′-cG^{s}AMP) or the 2′-5′-phosphodiester bond (**105**, 2′,3′-cGA^{s}MP) or both (**106**, 2′,3′-cG^{s}A^{s}MP) with phosphothioate linkage (Fig. 25). It is found the 2′,3′-cG^{s}A^{s}MP is the most stable in THP-1 cell lysates and is ∼40 times more resistant to ENPP1 hydrolysis than 2′,3′-cGAMP. Therefore, 2′,3′-cG^{s}A^{s}MP (**106**) is worthy for further investigation either as a vaccine adjuvant or as a new cancer treatment.

Recently, the structure of ENPP1 in complex with 3′,3′-cGAMP is reported (Fig. 26), providing more mechanism insights on how this enzyme adopts a conformation to specifically bind and hydrolyze 2′,3′-cGAMP[100]. A single active site of ENPP1 is proposed to preferentially recognize the adenine and guanine bases in the N-pocket and G-pocket, respectively, which then initiate the sequential degradation of the two distinct 2′-5′- and 3′-5′-phosphodiester bonds in 2′,3′-cGAMP. This result will be useful for further elucidation of the degradation mechanism by ENPP1 and provides insights to design drug-like ENPP1 inhibitors for *in vivo* study.

5. Clinical status of the cGAS−STING−TBK1 modulators

5.1. *ADU-S100 (Table 1)*

This compound is the earliest STING agonist that enters in human clinical trial developed by Aduro Biotech as stimulatory immunotherapy for cancers. It is a CDN analogue of the endogenous agonist 2′,3′-cGAMP containing 2′-3′- and 3′-5′-thiophosphodiester linkages on the c-di-AMP scaffold. It is designed to enhance resistance to ENPP1-mediated degradation, resulting in prolonged systemic half-life time while maintaining elevated activation of STING. I.t. injection of ADU-S100 in several syngeneic mouse models has showed significant anti-tumor immunity with tumor regression, long-lived immunologic memory, and suppression of distant metastases. In March 2015, Aduro entered into a worldwide agreement with Novartis for the joint research, development and commercialization of ADU-S100. Although many aspects of the activation mechanism are unclear, based on

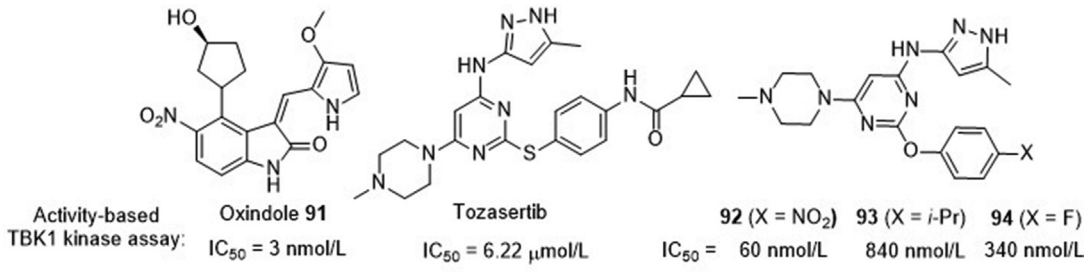

Figure 21 TBK1 inhibitors **91**−**94**.

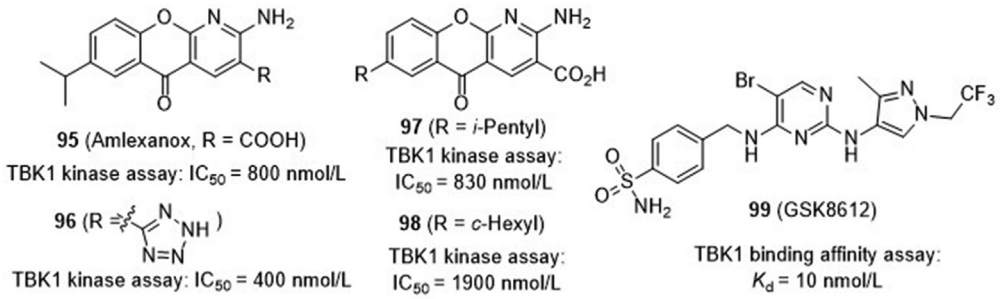

Figure 22 TBK1 inhibitors **95**–**99**.

the exciting preclinical results, ADU-S100 has been aggressively launched into phase I clinical trials since 2016 for patients with advanced metastatic solid tumors or lymphomas alone or in combination with anti-CTAL-4 monoclonal antibody ipilimumab (NCT02675439) or with an anti-PD-1 monoclonal antibody spartalizumab (NCT03172936). Partial results from ongoing phase Ib show that ADU-S100 in combination with spartalizumab demonstrates anti-tumor activity without dose-limiting toxicities (DLT) in triple-negative breast cancer (TNBC) and melanoma previously treated by immunotherapy (data cut-off: April 5, 2019). One of the eight TNBC patients for efficacy evaluation has achieved a complete response, and two have showed partial responses. Two of 25 melanoma patients previously treated by immunotherapy attain partial responses. The five confirmed responders achieve the median reduction of 73% in the target lesion diameters. Pharmacokinetic study indicated the absorption of ADU-S100 from injection site was rapid within minutes, and its plasma exposure increased in a dose-dependent manner from 50 to 800 ug. The systemic clearance from circulation was also quick with a terminal half-life of approximately 10–23 min. 78% of patients displayed treatment-related adverse events (TRAEs), of which 12.2% were relatively serious grade 3/4. The most common (>or = 10% of patients) TRAEs were pyrexia, injection site pain and headache. Grade 3/4 TRAEs mainly included increased lipase (3.6%), diarrhea, and elevated AST and ALT (2.4% each). Maximum tolerated dose was not reached due to established with the increased lipase. Overall, the toxicity profile of ADU-S100 was manageable. More complete data is expected available in 2020. Very recently, Novartis and Aduro BioTech launched a phase II efficacy and safety trial of ADU-S100 as the first line in combination with pembrolizumab in 33 patients with PD-L1 positive recurrent or metastatic head and neck squamous cell carcinoma (HNSCC) in the US (NCT03937141). The clinical trial is estimated to be completed in 2022. However, in December 2019, Aduro and Novartis terminated the clinical trials of ADU-S100 based on the disappointing clinical efficacy, and their decision was believed not to be the result of any safety concern.

5.2. *MK-1454*

The drug candidate MK-1454 is another synthetic CDN analogue with structure unknown that is developed by Merck & Co. for the treatment of advanced/metastatic solid tumors or lymphomas. Currently, it is undergoing phase I trial as monotherapy and in combination with PD-1 inhibitor pembrolizumab (NCT03010176). Interim data shows that MK-1454, as a single agent, is able to boost pro-inflammatory cytokines, but no complete or partial responses (n = 0/20) has been achieved in the monotherapy group. The combination arm with pembrolizumab shows overall response rate up to 24% with median reductions of 83% in the size of the target tumor. Pharmacokinetic study demonstrated the plasma exposure of MK-1454 increased in a dose-dependent manner with a half-life time of 1.5 h in the circulation. In both the monotherapy and

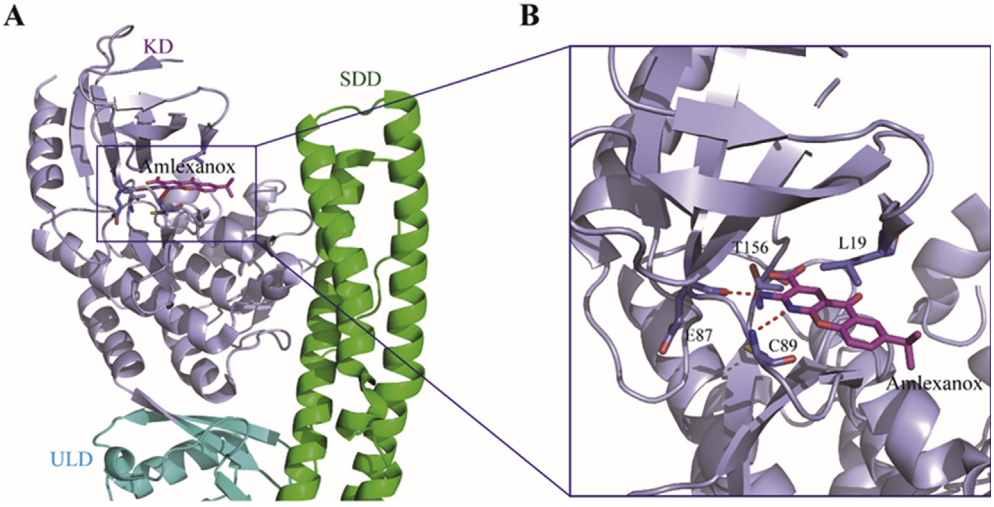

Figure 23 Co-crystal structure of human TBK1 bound with **95** (amlexanox, PDB ID: 5W5V). The TBK1 and **95** are depicted in purple and magenta, respectively, and H-bond interactions in the hinge region of TBK1 are depicted as red dashed lines.

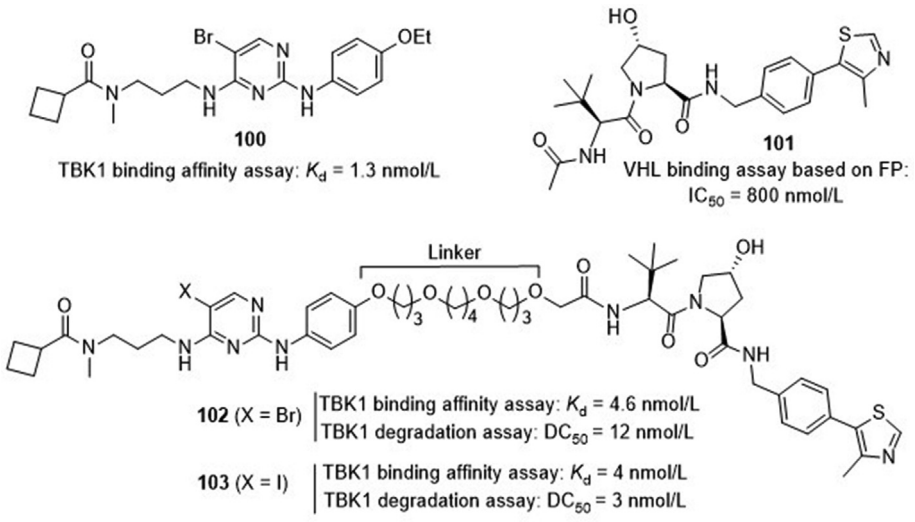

Figure 24 TBK1 PROTACs **102** and **103**.

combination arms, treatment related adverse events (TRAEs) are 82.6% and 82.1%, respectively. Three DLTs were observed including vomiting at 1500 μg monotherapy, erythema multiforme at 540 μg as well as injection site pain or tumor necrosis at 1500 μg in combination. Severe TRAEs leading to trial discontinuation were observed in 7.1% of patients in the combination therapy. However, there is no TRAE discontinuation in the monotherapy arm. The complete results are proposed to be released in 2021.

5.3. *MK-2118*

In 2017, Merck & Co. launched another phase I clinical trial of a STING agonist MK-2118 in combination with pembrolizumab for the treatment of solid tumors or lymphomas (NCT03249792) to assess its safety, tolerability, maximum tolerated or suggested phase II doses. The first result is expected in 2021. However, the structure of MK-2118 is unknown.

5.4. *BMS-986301*

The candidate BMS-986301 is a synthetic STING agonist originally developed by IFM Therapeutics, which was later acquired by Bristol-Myers Squibb. In CT26 or MC38 mouse models, monotherapy of BMS-986301 at the dose of 250 μg (Q4D × 3) shows 90% complete regressions, whereas the same dose of ADU-S100 provides only 13% complete regressions. In CT26 model, the combination of BMS-986301 with anti-PD-1 monoclonal antibody provides 80% complete regressions, while no complete regressions are achieved when treated with anti PD-1 alone. All CT26 mice with complete tumor regressions are found to generate immunological memory to reject fresh tumor cells without further treatment. Currently, BMS-986301 is in phase I trial (CA046-006, NCT03956680) in both Canada and the USA under development by Bristol-Myers Squibb as a monotherapy and in combination with nivolumab and ipilimumab for treating advanced solid cancers. However, the structure of BMS-986301 has not been disclosed yet.

5.5. *GSK-3745417*

The drug candidate GSK-3745417, developed by GlaxoSmithKline, is believed to be a synthetic non-CDN STING agonist with dimeric ABZI scaffold suitable for systemic administration. Intravenous administration of GSK-3745417 to immunologically active mice bearing syngeneic colon tumors elicits strong antitumor immunity with complete and lasting regression of tumors. Since 2019, GSK-3745417 has been launched by GlaxoSmithKline into phase I clinical trial in 300 participants with refractory/relapsed solid tumors to assess the safety, tolerability, and preliminary clinical efficacy, as well as to establish an optimal i.v. dose for GSK3745417 alone or co-administered with pembrolizumab (NCT03843359). The first result of this trial is expected to be disclosed in 2022. So far, the exact chemical structure of GSK-3745417 is not disclosed.

5.6. *SB-11285*

The drug candidate SB-11285 is a small molecule-nucleic acid hybrid STING agonist developed by Spring Bank Pharmaceuticals for the potential treatment of cancer and viral infections. It could cause STING-dependent inductions of IRF and NF-κB with EC_{50} values of 2 and 200 nmol/L, respectively, which were at least 200-fold more potent than 2′,3′-cGAMP. *In vivo* study showed that SB-11285 in combination with cyclophosphamide demonstrated durable and potent anti-tumor response in A20 and CT26 syngeneic

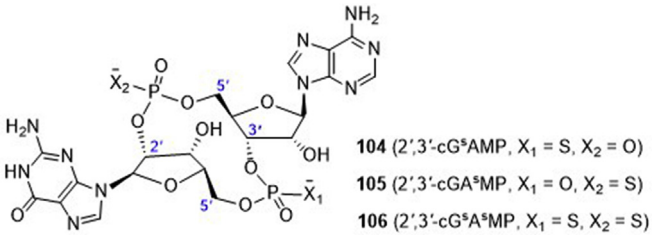

Figure 25 Phosphothioate analogues of 2′,3′-cGAMP.

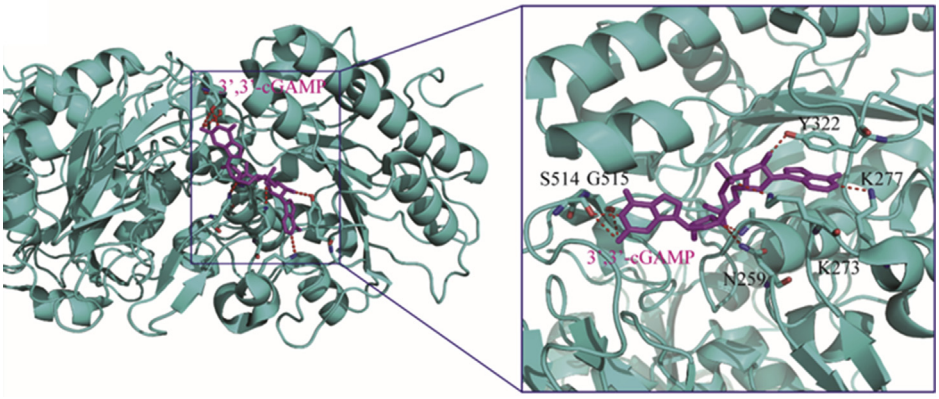

Figure 26 Co-crystal structure of mouse ENPP1 in complex with 3′,3′-cGAMP (PDB ID: 6AEL). ENPP1 and 3′,3′-cGAMP are depicted in cyan and magenta, respectively, and H-bonds in the complex are depicted as red dashed lines.

mouse tumor models upon intra-tumoral, intraperitoneal or i.v. administration, and the SB-11285-treated groups displayed $CD8^+$T- and NK cell infiltration into the tumor and surrounding tissues without systemic inflammatory response. Based on the preclinical data, a phase Ia/Ib trial in patients (expected $n = 110$) with advanced solid tumors including melanoma and head and neck squamous cell carcinoma was planned to begin in the USA to examine the efficacy of SB-11285 in combination with nivolumab in September 2019 (NCT04096638), and the trial result is expected in 2020. The structure of BMS-986301 has not been disclosed yet.

Table 1 STING agonists currently in clinical trials.

Drug name	Developer	Status	Study start date	Content of clinical trials
ADU-S100 (compd. **1**)	Novartis (Aduro Biotech)	Trial termination	Dec 2019	Clinical trials of ADU-S100 was terminated by Novartis due to lack of enough activity or efficacy
		Phase II	Jun 2019	NCT03937141: efficacy and safety trial of ADU-S100 in combination with anti-PD1 monoclonal antibody in head and neck cancer
		Phase Ib	Sep 2017	NCT02675439: safety and efficacy of ADU-S100 with spartalizumab on patients with advanced/metastatic solid tumors or lymphomas
		Phase I	Mar 2016	NCT03172936: safety and efficacy of ADU-S100 alone or in combination with ipilimumab in patients with advanced/metastatic solid tumors or lymphomas
MK-1454 (structure not disclosed)	Merck & Co.	Phase I	Feb 2017	NCT03010176: safety and efficacy of MK-1454 alone or in combination with pembrolizumab in participants with advanced/metastatic solid tumors or lymphomas
MK-2118 (structure not disclosed)	Merck & Co.	Phase I	Sep 2017	NCT03249792: safety and efficacy of MK-2118 administered intratumorally alone or in combination with pembrolizumab or co-administered subcutaneously with pembrolizumab for patients with advanced/metastatic solid tumors or lymphomas
BMS-986301 (structure not disclosed)	Bristol-Myers Squibb	Phase I	Mar 2019	NCT03956680: safety and efficacy of BMS-986301 alone or co-administered with nivolumab and ipilimumab to participants with advanced solid cancers
GSK3745417 (structure not disclosed)	GlaxoSmithKline	Phase I	Mar 2019	NCT03843359: safety and efficacy of GSK3745417 administered intravenously alone or in combination with pembrolizumab in participants with advanced solid tumors
SB-11285 (structure not disclosed)	Spring Bank Pharmaceuticals	Phase I	Sep 2019	NCT04096638: safety, tolerability and initial anti-tumor activity of SB-11285 in combination with nivolumab in participants with advanced solid tumors
IMSA-101 (structure not disclosed)	ImmuneSensor Therapeutics Inc.	Phase I/II	Sep 2019	NCT04020185: safety and efficacy of IMSA-101 alone or in combination with ICIs in patients with advanced solid tumors

Searched through Biomedtracker at https://pharma.id.informa.com on Jan 10, 2020.

5.7. *IMSA-101*

IMSA-101 is an analog of cGAMP developed by ImmuneSensor Therapeutics as the small molecule STING agonist. In preclinical studies, it demonstrated highly effective anti-tumor activity alone or co-administrated with checkpoint inhibitors for the potential i.t. treatment of advanced solid tumors resistant to anti-PD-1/-L1 monoclonal antibodies. An open-label and non-randomized phase I/II trial was initiated in September 2019 to assess the safety and therapeutic efficacy of IMSA-101 alone or in combination with ICIs as dose escalation (phase I) and dose expansion (phase IIa) in patients (expected $n = 115$) with advanced solid tumors (NCT04020185). The trial is expected to complete in 2023. The chemical structure of GSK-3745417 is not known.

As mentioned in the previous paragraphs, the researches on cGAS−STING−TBK1 inhibitors have mainly focused on the preclinical stage, and no inhibitor has been launched into the clinical trials yet. Nevertheless, we believe that there will be clinical trials of these inhibitors to be carried out in the near future.

6. Conclusions and perspectives

Thanks to the rapid evolution of tumor basic biology and clinical treatment practice, therapeutic modalities against cancer have been advanced from radiation therapy, hormonal manipulation, cytotoxic chemotherapy, and targeted therapy, which all focus on the constantly proliferative cancer cell itself, to current immunotherapy that kills cancer cells indirectly by harnessing the host's innate and adaptive immune system. Antibodies targeting the immunosuppressive checkpoint molecules CTLA-4 and PD-1/PD-L1 have met great success and the 2018 Nobel Prize in Medicine and Physiology has been awarded to James P. Allison and Tasuku Honjo to acknowledge their discovery of immune-oncology (IO) therapy.

Indeed, IO therapy has now become an established pillar treatment for hematological and solid malignancies with curable potentials for certain tumors[101]. However, many challenges and limitations are increasingly raised during the clinical practice. Particularly, only one quarter of patients effectively respond to PD-1/PD-L1 blockers and an effective biomarker to predict and stratify potential responders is still lacked[101,102]. Therefore, precise immunotherapy is far beyond our reach. It is found that many non-responsive tumors treated by ICIs are immunologically non-inflamed "cold" tumors (lack of T celll infiltration, or low or absent of chemokine expression), and might be reversed to be active responders of ICIs by stimulating immune cells infiltration to "heat up" the "cold" tumors[103−106]. Among these strategies, activation of the cGAS–STING–TBK1 signaling pathway to stimulate the innate immune system and enhance tumor immunogenicity has been found as the most promising approach.

The cGAS–STING–TBK1 axis is initially recognized as the essential mechanism for the host to defeat bacteria and virus invasions, and is now believed as the major innate immune pathway implicated in the generation of spontaneous anti-tumor T cell response by sensing tumor-derived dsDNA. Among this pathway, cGAS is the critical enzyme to sense DNA dangerous signals from pathogens, cancer or cellular breakdown and trigger the fast-acting innate immune response. The free cGAS exists as a dimer to bind two molecules of dsDNA in "head-to-head" orientation to form a ladder-like network and induce a significant conformational change in the NTase domain, leading to a structural switch of the catalytic pocket to allow binding of ATP and GTP for the synthesis of 2′,3′-cGAMP. The produced 2′,3′-cGAMP then acts as the specific endogenous high potent agonist of STING. The dimeric V-shaped apo-STING binds one molecule of 2′,3′-cGAMP in the dimeric interface, leading to a "closed" conformation in the "lid" loop. STING is then activated by formation of stable oligomers with the CTT released. The PLPLRT/SD motif in the CTT of STING oligomers binds with the interface of dimeric TBK1 to induce phosphorylation and activation of both STING and TBK1, thus eventually leading to engagement of downstream signaling components and induction of type I IFN transcription, a hallmark signaling of the cGAS–STING–TBK1 pathway.

Although development of cGAS and TBK1 activators is reasonable and potentially useful, activation of the cGAS–STING–TBK1 signaling pathway has mainly focused on STING agonistic approach[25,35,107,108]. Earlier efforts have provided a CDN analogue ADU-S100 that is more enzymatically stable than the endogenous ligand 2′,3′-cGAMP, and is found to show appealing tumor suppressing effect and sustain immune memory in preclinical mice model through i.t. injection. ADU-S100 and another CDN analogue MK-1454 are now in a number of clinical trials. Small molecule STING agonists have also been pursued and GSK-3745417, one of the dimeric ABZIs, is the first small molecule suitable for systemic administration and has recently been investigated in human clinical study. Although several other STING agonists, either CDN analogues or small molecules, are also claimed to undergo clinical trials, their structures have not been decoded yet. In addition, inhibitors of cGAS, STING and TBK1 have also attracted more and more interests, but their application in human diseases need to be further explored. Meanwhile, in addition to directly stimulating STING itself, inhibition of phosphodiesterase ENPP1, a key negative regulator of the STING pathway is an alternative appealing approach to show controllable enhancement of STING signalling in certain tumoral models. Indeed, a small molecule MAVU-104 (structure is unknown) developed by Mavupharm is claimed as the first-in-class orally active ENPP1 inhibitor to initiate clinical trial later this year.

Despite the high enthusiasm and rapid progress in drug discovery of the cGAS–STING–TBK1 signaling pathway, our understanding and capability for modulating this pathway are still at the early stage, and there are more questions and challenges than answers. On one hand, although the advance in the structural biology has essentially enhanced our understanding on the activation mechanism and interaction network of this pathway, yet how cGAS selectively senses dangerous dsDNA from the abundant other DNA (self DNA, ssDNA, etc.) and cellular molecules is unclear. Also, how and by what means the endogenous 2′,3′-cGAMP after synthesis by cGAS transitions and specifically binds to STING is of no firm clues. Meanwhile, our understanding on the 2′,3′-cGAMP-binding-induced STING activation is insufficient without consideration of the CTD since it is buried in the back of the currently reported ligand−STING complex structures, which is also importantly involved in the activation mechanism. In addition, it is not for sure that how and when the activated STING traffics from the ER membrane to Golgi, upon or after binding with TBK1. On the other hand, although quite optimistic, clinical use of STING activators needs to be cautious. According to the interim data from ongoing phase I clinical trials, STING agonists elicit disappointingly modest efficacy. Therefore, combination

therapy of STING agonists with checkpoint inhibitors may achieve higher overall response than monotherapy. Some modified CDN analogues have been aggressively advanced into clinical studies, but their clinical applications might be soaked by their poor druglikeness and costive drug delivery techniques. The small molecule non-CDN STING agonists open a new avenue to achieve systemic administration of the drug, but no clinical data has been released yet. A more serious concern on the stimulant immune therapy is the risk of potential "cytokine storm". The continuing activation of STING may lead to the excessive production of cytokines that are severely toxic and even deadly, but so far little is known on whether this is true in clinic and how to properly shut down the activated signaling to prevent the "cytokine storm" once it is triggered[109,110]. Therefore, it is too early to draw any conclusion on how much the tumor-bearing patients will benefit from the stimulant immune therapy, and much more effort on all aspects of the cGAS–STING–TBK1 signaling pathway is needed.

Acknowledgments

This work was supported by grants from Natural Science Foundation of China (Nos. 81773565, 21877120, 81703327, 81430080, 81573452, and 81773767, China). Supporting grants from the Key Program of the Frontier Science of the Chinese Academy of Sciences (No. 160621, China), the Strategic Priority Research Program of the Chinese Academy of Sciences (No. XDA12020374, China), and a start-up grant to the Research Laboratory of Medicinal Chemical Biology & Frontiers on Drug Discovery from Shanghai Jiao Tong University (China) are also appreciated.

Author contributions

Ao Zhang, Chunyong Ding, and Zilan Song have jointly written the manuscript based on an intense literature survey conducted by Ancheng Shen. Ao Zhang and Tingting Chen made the figures. Chunyong Ding, Zilan Song and Ancheng Shen reviewed and edited the manuscript. Ao Zhang supervised the manuscript.

Conflicts of interest

Authors declare absence of conflict of interest.

References

1. Takeuchi O, Akira S. Pattern recognition receptors and inflammation. *Cell* 2010;**140**:805−20.
2. Lesterhuis WJ, Haanen JB, Punt CJ. Cancer immunotherapy—revisited. *Nat Rev Drug Discov* 2011;**10**:591−600.
3. Hanahan D, Weinberg RA. Hallmarks of cancer: the next generation. *Cell* 2011;**144**:646−74.
4. Li Z, Song W, Rubinstein M, Liu D. Recent updates in cancer immunotherapy: a comprehensive review and perspective of the 2018 China Cancer Immunotherapy Workshop in Beijing. *J Hematol Oncol* 2018;**11**:142−56.
5. Kruger S, Ilmer M, Kobold S, Cadilha BL, Endres S, Ormanns S, et al. Advances in cancer immunotherapy 2019—latest trends. *J Exp Clin Cancer Res* 2019;**38**:268−78.
6. Sondak VK, Smalley KS, Kudchadkar R, Grippon S, Kirkpatrick P. Ipilimumab. *Nat Rev Drug Discov* 2011;**10**:411−2.
7. Tan M, Quintal L. Pembrolizumab: a novel antiprogrammed death 1 (PD-1) monoclonal antibody for treatment of metastatic melanoma. *J Clin Pharm Ther* 2015;**40**:504−7.
8. Mashima E, Inoue A, Sakuragi Y, Yamaguchi T, Sasaki N, Hara Y, et al. Nivolumab in the treatment of malignant melanoma: review of the literature. *OncoTargets Ther* 2015;**8**:2045−51.
9. Adams JL, Smothers J, Srinivasan R, Hoos A. Big opportunities for small molecules in immuno-oncology. *Nat Rev Drug Discov* 2015;**14**:603−22.
10. Dhanak D, Edwards JP, Nguyen A, Tummino PJ. Small-molecule targets in immuno-oncology. *Cell Chem Biol* 2017;**24**:1148−60.
11. Huck BR, Kötzner L, Urbahns K. Small molecules drive big improvements in immuno-oncology therapies. *Angew Chem Int Ed* 2018;**57**:4412−28.
12. Cheng B, Yuan WE, Su J, Liu Y, Chen J. Recent advances in small molecule based cancer immunotherapy. *Eur J Med Chem* 2018;**157**:582−98.
13. Weinmann H. Cancer immunotherapy: selected targets and small-molecule modulators. *ChemMedChem* 2016;**11**:450−66.
14. Gong J, Chehrazi-Raffle A, Reddi S, Salgia R. Development of PD-1 and PD-L1 inhibitors as a form of cancer immunotherapy: a comprehensive review of registration trials and future considerations. *J Immunother Cancer* 2018;**6**:8−25.
15. Tang J, Yu JX, Hubbard-Lucey VM, Neftelinov ST, Hodge JP, Lin Y. Trial watch: the clinical trial landscape for PD1/PDL1 immune checkpoint inhibitors. *Nat Rev Drug Discov* 2018;**17**:854−5.
16. Chen S, Song Z, Zhang A. Small-molecule immuno-oncology therapy: advances, challenges and new directions. *Curr Top Med Chem* 2019;**19**:180−5.
17. Fritz JM, Lenardo MJ. Development of immune checkpoint therapy for cancer. *J Exp Med* 2019;**216**:1244−54.
18. Zhang H, Chen J. Current status and future directions of cancer immunotherapy. *J Cancer* 2018;**9**:1773−81.
19. Mazzarella L, Duso BA, Trapani D, Belli C, D'Amico P, Ferraro E, et al. The evolving landscape of 'next-generation' immune checkpoint inhibitors: a review. *Eur J Cancer* 2019;**117**:14−31.
20. Torphy RJ, Schulick RD, Zhu Y. Newly emerging immune checkpoints: promises for future cancer therapy. *Int J Mol Sci* 2017;**18**:2642.
21. Dempke WC, Fenchel K, Uciechowski P, Dale SP. Second- and third-generation drugs for immuno-oncology treatment—the more the better?. *Eur J Cancer* 2017;**74**:55−72.
22. Wolchok J. Putting the immunologic brakes on cancer. *Cell* 2018;**175**:1452−4.
23. van der Woude LL, Gorris MA, Halilovic A, Figdor CG, de Vries IJM. Migrating into the tumor: a roadmap for T cells. *Trends Cancer* 2017;**3**:797−808.
24. Mayes PA, Hance KW, Hoos A. The promise and challenges of immune agonist antibody development in cancer. *Nat Rev Drug Discov* 2018;**17**:509−27.
25. Li A, Yi M, Qin S, Song Y, Chu Q, Wu K. Activating cGAS−STING pathway for the optimal effect of cancer immunotherapy. *J Hematol Oncol* 2019;**12**:35−46.
26. Corrales L, McWhirter SM, Dubensky Jr TW, Gajewski TF. The host STING pathway at the interface of cancer and immunity. *J Clin Invest* 2016;**126**:2404−11.
27. Burdette DL, Vance RE. STING and the innate immune response to nucleic acids in the cytosol. *Nat Immunol* 2013;**14**:19−26.
28. Ishikawa H, Ma Z, Barber GN. STING regulates intracellular DNA-mediated, type I interferon-dependent innate immunity. *Nature* 2009;**461**:788−93.
29. Barber GN. STING-dependent cytosolic DNA sensing pathways. *Trends Immunol* 2014;**35**:88−93.
30. Barber GN. STING: infection, inflammation and cancer. *Nat Rev Immunol* 2015;**15**:760−70.
31. Vargas TR, Benoit-Lizon I, Apetoh L. Rationale for stimulator of interferon genes-targeted cancer immunotherapy. *Eur J Cancer* 2017;**75**:86−97.
32. Sun L, Wu J, Du F, Chen X, Chen ZJ. Cyclic GMP−AMP synthase is a cytosolic DNA sensor that activates the type I interferon pathway. *Science* 2013;**339**:786−91.

33. Motwani M, Pesiridis S, Fitzgerald KA. DNA sensing by the cGAS-STING pathway in health and disease. *Nat Rev Genet* 2019;**20**:657−74.
34. Ablasser A, Chen ZJ. cGAS in action: expanding roles in immunity and inflammation. *Science* 2019;**363**:eaat8657.
35. Bai J, Liu F. The cGAS-cGAMP-STING Pathway: a molecular link between immunity and metabolism. *Diabetes* 2019;**68**:1099−108.
36. Kato K, Omura H, Ishitani R, Nureki O. Cyclic GMP−AMP as an endogenous second messenger in innate immune signaling by cytosolic DNA. *Annu Rev Biochem* 2017;**86**:541−66.
37. Andreeva L, Hiller B, Kostrewa D, Lässig C, de Oliveira Mann CC, Jan Drexler D, et al. cGAS senses long and HMGB/TFAM-bound U-turn DNA by forming protein-DNA ladders. *Nature* 2017;**549**:394−8.
38. Gao P, Ascano M, Wu Y, Barchet W, Gaffney BL, Zillinger T, et al. Cyclic [G (2′,5′) pA (3′,5′) p] is the metazoan second messenger produced by DNA-activated cyclic GMP-AMP synthase. *Cell* 2013;**153**:1094−107.
39. Civril F, Deimling T, de Oliveira Mann CC, Ablasser A, Moldt M, Witte G, et al. Structural mechanism of cytosolic DNA sensing by cGAS. *Nature* 2013;**498**:332−7.
40. Patel S, Jin L. TMEM173 variants and potential importance to human biology and disease. *Genes Immun* 2019;**20**:82−9.
41. Shang G, Zhu D, Li N, Zhang J, Zhu C, Lu D. Crystal structures of STING protein reveal basis for recognition of cyclic di-GMP. *Nat Struct Mol Biol* 2012;**19**:725−7.
42. Shang G, Zhang C, Chen ZJ, Bai X, Zhang X. Cryo-EM structures of STING reveal its mechanism of activation by cyclic GMP-AMP. *Nature* 2019;**567**:389−93.
43. Ergun SL, Fernandez D, Weiss TM, Li L. STING Polymer structure reveals mechanisms for activation, hyperactivation, and inhibition. *Cell* 2019;**178**:290−301.
44. Li J, Li J, Miyahira A, Sun J, Liu Y, Cheng G, et al. Crystal structure of the ubiquitin-like domain of human TBK1. *Protein Cell* 2012;**3**:383−91.
45. Larabi A, Devos JM, Ng SL, Nanao MH, Round A, Maniatis T, et al. Crystal structure and mechanism of activation of TANK-binding kinase 1. *Cell Rep* 2013;**3**:734−46.
46. Zhao C, Zhao W. TANK-binding kinase 1 as a novel therapeutic target for viral diseases. *Expert Opin Ther Targets* 2019;**23**:437−46.
47. Zhang C, Shang G, Gui X, Zhang X, Bai XC, Chen ZJ. Structural basis of STING binding with and phosphorylation by TBK1. *Nature* 2019;**567**:394−414.
48. Zhao B, Du F, Xu P, Shu C, Sankaran B, Bell SL, et al. A conserved PLPLRT/SD motif of STING mediates the recruitment and activation of TBK1. *Nature* 2019;**569**:718−39.
49. Gajewski TF. The next hurdle in cancer immunotherapy: overcoming the non-T-cell-inflamed tumor microenvironment. *Semin Oncol* 2015;**42**:663−71.
50. Kerr WG, Chisholm JD. The Next Generation of immunotherapy for cancer: small molecules could make big waves. *J Immunol* 2019;**202**:11−9.
51. Cui X, Zhang R, Cen S, Zhou J. STING modulators: predictive significance in drug discovery. *Eur J Med Chem* 2019;**182**:111591−605.
52. Berger G, Marloye M, Lawler SE. Pharmacological modulation of the STING pathway for cancer immunotherapy. *Trends Mol Med* 2019;**25**:412−27.
53. Zhang X, Shi H, Wu J, Zhang X, Sun L, Chen C, et al. Cyclic GMP-AMP containing mixed phosphodiester linkages is an endogenous high-affinity ligand for STING. *Mol Cell* 2013;**51**:226−35.
54. Deng L, Liang H, Xu M, Yang X, Burnette B, Arina A, et al. STING-dependent cytosolic DNA sensing promotes radiation-induced type I interferon-dependent anti-tumor immunity in immunogenic tumors. *Immunity* 2014;**41**:843−52.
55. Li T, Cheng H, Yuan H, Xu Q, Shu C, Zhang Y, et al. Anti-tumor activity of cGAMP *via* stimulation of cGAS-cGAMP-STING-IRF3 mediated innate immune response. *Sci Rep* 2016;**6**:19049−62.
56. Corrales L, Glickman LH, McWhirter SM, Kanne DB, Sivick KE, Katibah GE, et al. Direct activation of STING in the tumor microenvironment leads to potent and systemic tumor regression and immunity. *Cell Rep* 2015;**11**:1018−30.
57. Lioux T, Mauny MA, Lamoureux A, Bascoul N, Hays M, Vernejoul F, et al. Design, synthesis, and biological evaluation of novel cyclic adenosine−inosine monophosphate (cAIMP) analogs that activate stimulator of interferon genes (STING). *J Med Chem* 2016;**59**:10253−67.
58. Dialer CR, Stazzoni S, Drexler DJ, Muller FM, Veth S, Pichler A, et al. A click-chemistry linked 2′,3′-cGAMP analogue. *Chem Eur J* 2019;**25**:2089−95.
59. Prantner D, Perkins DJ, Lai W, Williams MS, Sharma S, Fitzgerald K, et al. 5,6-Dimethylxanthenone-4-acetic acid (DMXAA) activates stimulator of interferon gene (STING)-dependent innate immune pathways and is regulated by mitochondrial membrane potential. *J Biol Chem* 2012;**287**:39776−88.
60. Gao P, Ascano M, Zillinger T, Wang W, Dai P, Serganov AA, et al. Structure-function analysis of STING activation by c [G (2′,5′) pA (3′,5′) p] and targeting by antiviral DMXAA. *Cell* 2013;**154**:748−62.
61. Gao P, Zillinger T, Wang W, Ascano M, Dai P, Hartmann G, et al. Binding-pocket and lid-region substitutions render human STING sensitive to the species-specific drug DMXAA. *Cell Rep* 2014;**8**:1668−76.
62. Hwang J, Kang T, Lee J, Choi BS, Han S. Design, synthesis, and biological evaluation of *C*7-functionalized DMXAA derivatives as potential human-STING agonists. *Org Biomol Chem* 2019;**17**:1869−74.
63. Cavlar T, Deimling T, Ablasser A, Hopfner KP, Hornung V, et al. Species-specific detection of the antiviral small molecule compound CMA by STING. *EMBO J* 2013;**32**:1440−50.
64. Liu B, Tang L, Zhang X, Ma J, Sehgal M, Cheng J, et al. A cell-based high throughput screening assay for the discovery of cGAS−STING pathway agonists. *Antivir Res* 2017;**147**:37−46.
65. Sali TM, Pryke KM, Abraham J, Liu A, Archer I, Broeckel R, et al. Characterization of a novel human-specific STING agonist that elicits antiviral activity against emerging alphaviruses. *PLoS Pathog* 2015;**11**:e1005324.
66. Zhang Y, Sun Z, Pei J, Luo Q, Zeng X, Li Q, et al. Identification of α-mangostin as an agonist of human STING. *ChemMedChem* 2018;**13**:2057−64.
67. Zhang X, Liu B, Tang L, Su Q, Hwang N, Sehgal M, et al. Discovery and mechanistic study of a novel human-stimulator-of-interferon-genes agonist. *ACS Infect Dis* 2019;**5**:1139−49.
68. Ramanjulu JM, Pesiridis GS, Yang J, Concha N, Singhaus R, Zhang S, et al. Design of amidobenzimidazole STING receptor agonists with systemic activity. *Nature* 2018;**564**:439−54.
69. Li J, Zhang D, Wei Y, Pan F, Ma R, Li Y, et al., inventors; GlaxoSmithKline, assignee. *Immunomodulator.* PCT Int Appl. WO 2019134705 A1. July 11, 2019. p. 1−87.
70. Banerjee M, Middya S, Basu S, Ghosh R, Pryde D, Yadav D, et al., inventors. Curde Pharm, assignee. *Small molecule modulators of human STING*. PCT Int Appl. WO 2018234805 A1. Dec 27, 2018. p. 1−234.
71. Banerjee M, Middya S, Basu S, Ghosh R, Pryde D, Yadav D, et al., inventors. Curde Pharm, assignee. *Small molecule modulators of human STING*. PCT Int Appl. WO 2018234808 A1. Dec 27, 2018. p. 1−283.
72. Banerjee M, Middya S, Basu S, Yadav D, Ghosh R, Pryde D, et al., inventors. Curde Pharm, assignee. *Heterocyclic small molecule modulators of human STING*. PCT Int Appl. WO 2018234807 A1. Dec 27, 2018. p. 1−176.
73. Altman MD, Cash BD, Chang W, Cumming JN, Haidle AM, Henderson TJ, et al., inventors. Merck Sharp & Dohme Corp., assignee. *Benzo[b]thiophene compounds as STING agonists*. PCT Int Appl. WO 2018067423 A1. Apr 12, 2018. p. 1−185.
74. Cemerski S, Cumming JN, Kopinja JE, Perera SA, Trotter BW, Tse ANC, inventors. Merck, assignee. *Benzo[b]thiophene STING*

agonists for cancer treatment. PCT Int Appl. WO 2019027858 A1. Feb 07, 2019. p. 1−56.
75. Cemerski S, Cumming JN, Kopinja JE, Perera SA, Trotter BW, Tse ANC, inventors. Merck Sharp & Dohme Corp., assignee. *Combinations of PD-1 antagonists and benzo[b]thiophene STING agonists for cancer treatment*. PCT Int Appl. WO 2019027857 A1. Feb 07, 2019. p. 1−73.
76. Siu T, Altman MD, Baltus GA, Childers M, Ellis JM, Gunaydin H, et al. Discovery of a novel cGAMP competitive ligand of the inactive form of STING. *ACS Med Chem Lett* 2018;**10**:92−7.
77. Haag SM, Gulen MF, Reymond L, Gibelin A, Abrami L, Decout A, et al. Targeting STING with covalent small molecule inhibitors. *Nature* 2018;**559**:269−90.
78. Li S, Hong Z, Wang Z, et al. The cyclopeptide astin C specifically inhibits the innate immune CDN sensor STING. *Cell Rep* 2018;**25**: 3405−21.
79. Bose D, Su Y, Marcus A, Li F, Mei J, Huang L, et al. An RNA-based fluorescent biosensor for high-throughput analysis of the cGAS−GAMP−STING pathway. *Cell Chem Biol* 2016;**23**: 1539−49.
80. An J, Woodward JJ, Sasaki T, Raulet DH, Hammond MC. Cutting edge: antimalarial drugs inhibit IFN-β production through blockade of cyclic GMP-AMP synthase-DNA interaction. *J Immunol* 2015; **194**:4089−93.
81. An J, Woodward JJ, Lai W, Minie M, Sun X, Tanaka L, et al. Inhibition of cyclic GMP-AMP synthase using a novel antimalarial drug derivative in *Trex1*-deficient mice. *Arthritis Rheumatol* 2018;**70**: 1807−19.
82. Wang M, Sooreshjani MA, Mikek C, Opoku-Temeng C, Sintim HO. Suramin potently inhibits cGAMP synthase, cGAS, in THP1 cells to modulate IFN-β levels. *Future Med Chem* 2018;**10**:1301−17.
83. Vincent J, Adura C, Gao P, Luz A, Lama L, Asano Y, et al. Small molecule inhibition of cGAS reduces interferon expression in primary macrophages from autoimmune mice. *Nat Commun* 2017;**8**: 750−62.
84. Lama L, Adura C, Xie W, Tomita D, Kamei T, Kuryavyi V, et al. Development of human cGAS-specific small molecule inhibitors for repression of dsDNA-triggered interferon expression. *Nat Commun* 2019;**10**:2261−74.
85. Hall J, Brault A, Vincent F, Weng S, Wang H, Dumlao D, et al. Discovery of PF-06928215 as a high affinity inhibitor of cGAS enabled by a novel fluorescence polarization assay. *PLoS One* 2017; **12**:e0184843.
86. Ndubaku CO, Katibah GE, Roberts TC, Sung L, Ciblat S, Raeppel F, et al., inventors. Aduro Biotech, assignee. *Pyrazolopyrimidinone compounds and uses thereof*. PCT Int Appl. WO 2019055750 A1. Mar 21, 2019. p. 1−359.
87. Yu T, Yang Y, Yin DQ, Hong S, Son YJ, Kim JH, et al. TBK1 inhibitors: a review of patent literature (2011−2014). *Expert Opin Ther Pat* 2015;**25**:1385−96.
88. Clark K, Plater L, Peggie M, Cohen P. Use of the pharmacological inhibitor BX795 to study the regulation and physiological roles of TBK1 and IκB kinase ε: a distinct upstream kinase mediates Ser-172 phosphorylation and activation. *J Biol Chem* 2009;**284**:14136−46.
89. Clark K, Takeuchi O, Akira S, Cohen P. The TRAF-associated protein TANK facilitates cross-talk within the IκB kinase family during Toll-like receptor signaling. *Proc Natl Acad Sci U S A* 2011;**108**: 17093−8.
90. Lee SJ, Gharbi A, You JS, Han HD, Kang TH, Hong SH, et al. Drug repositioning of TANK-binding kinase 1 inhibitor CYT387 as an alternative for the treatment of Gram-negative bacterial sepsis. *Int Immunopharmacol* 2019;**73**:482−90.
91. Perrior TR, Newton GK, Stewart MR, Aqil R, inventors. Domainex Limited, assignee. *Pyrimidine compounds as inhibitors of protein kinases IKK epsilon and/or TBK-1, processes for their preparation, and pharmaceutical compositions containing them*. PCT Int Appl. WO 2012010826 A1. Jan 26, 2012. p. 1−65.
92. Li J, Huang J, Jeong JH, Park SJ, Wei R, Peng J, et al. Selective TBK1/IKKi dual inhibitors with anticancer potency. *Int J Cancer* 2014;**134**:1972−80.
93. Richters A, Basu D, Engel J, Ercanoglu MS, Balke-Want H, Tesch R, et al. Identification and further development of potent TBK1 inhibitors. *ACS Chem Biol* 2014;**10**:289−98.
94. Beyett TS, Gan X, Reilly SM, Chang L, Gomez AV, Saltiel AR, et al. Carboxylic acid derivatives of amlexanox display enhanced potency toward TBK1 and IKKε and reveal mechanisms for selective inhibition. *Mol Pharmacol* 2018;**94**:1210−9.
95. Beyett TS, Gan X, Reilly SM, Gomez AV, Chang L, Tesmer JJG, et al. Design, synthesis, and biological activity of substituted 2-amino-5-oxo-5*H*-chromeno[2,3-*b*]pyridine-3-carboxylic acid derivatives as inhibitors of the inflammatory kinases TBK1 and IKKε for the treatment of obesity. *Bioorg Med Chem* 2018;**26**:5443−6.
96. Thomson DW, Poeckel D, Zinn N, Rau C, Strohmer K, Wagner AJ, et al. Discovery of GSK8612, a highly selective and potent TBK1 inhibitor. *ACS Med Chem Lett* 2019;**10**:780−5.
97. Crew AP, Raina K, Dong H, Qian Y, Wang J, Vigil D, et al. Identification and characterization of Von Hippel-Lindau-recruiting proteolysis targeting chimeras (PROTACs) of TANK-binding kinase 1. *J Med Chem* 2017;**61**:583−98.
98. Kato K, Nishimasu H, Okudaira S, Mihara E, Ishitani R, Takagi J, et al. Crystal structure of Enpp1, an extracellular glycoprotein involved in bone mineralization and insulin signaling. *Proc Natl Acad Sci U S A* 2012;**109**:16876−81.
99. Li L, Yin Q, Kuss P, Maliga Z, Millan JL, Wu H, et al. Hydrolysis of 2′,3′-cGAMP by ENPP1 and design of nonhydrolyzable analogs. *Nat Chem Biol* 2014;**10**:1043−52.
100. Kato K, Nishimasu H, Oikawa D, Hirano S, Hirano H, Kasuya G, et al. Structural insights into cGAMP degradation by *ecto*-nucleotide pyrophosphatase phosphodiesterase 1. *Nat Commun* 2018;**9**: 4424−31.
101. Hargadon KM, Johnson CE, Williams CJ. Immune checkpoint blockade therapy for cancer: an overview of FDA-approved immune checkpoint inhibitors. *Int Immunopharmacol* 2018;**62**:29−39.
102. Salama AK, Moschos SJ. Next steps in immuno-oncology: enhancing anti-tumor effects through appropriate patient selection and rationally designed combination strategies. *Ann Oncol* 2016;**28**: 57−74.
103. Darvin P, Toor SM, Nair VS, Elkord E. Immune checkpoint inhibitors: recent progress and potential biomarkers. *Exp Mol Med* 2018;**50**:1−11.
104. Thorsson V, Gibbs DL, Brown SD, Wolf D, Bortone DS, Ou Yang T, et al. The immune landscape of cancer. *Immunity* 2018;**48**: 812−30.
105. O'Donovan DH, Mao Y, Mele DA. The next generation of pattern recognition receptor agonists: improving response rates in cancer immunotherapy. *Curr Med Chem* 2019;**26**:1−19.
106. Chen DS, Mellman I. Elements of cancer immunity and the cancer-immune set point. *Nature* 2017;**541**:321−30.
107. Sheridan C. Drug developers switch gears to inhibit STING. *Nat Biotechnol* 2019;**37**:199−201.
108. Ishikawa H, Barber GN. STING is an endoplasmic reticulum adaptor that facilitates innate immune signalling. *Nature* 2008;**455**:674−6.
109. Ng KW, Marshall EA, Bell JC, Lam WL. cGAS−STING and cancer: dichotomous roles in tumor immunity and development. *Trends Immunol* 2018;**39**:44−54.
110. Fu Y, Lin Q, Zhang Z, Zhang L. Therapeutic strategies for the costimulatory molecule OX40 in T-cell-mediated immunity. *Acta Pharm Sin B* 2020;**10**:414−33.